Sustainable Cities and Society 98 (2023) 104781

Contents lists available at ScienceDirect

Sustainable Cities and Society

journal homepage: www.elsevier.com/locate/scs

Improving occupational safety in office spaces in the post-pandemic era

Naimeh Sadeghi [a], Nima Gerami-Seresht [b,*]

[a] Department of Civil Engineering, K.N. Toosi University of Technology, Tehran, 19967-15433, Iran
[b] Department of Engineering, Durham University, South Road, Durham, DH1 3LE, United Kingdom

ARTICLE INFO

Keywords:
Occupational safety
COVID-19
Intervention
Infectious diseases
Agent-based modeling
Resilient workspace
Sustainability

ABSTRACT

The rise of COVID-19 and its consequent socio-economic losses raised concerns regarding the resilience of workplaces against widespread infectious diseases. During the COVID-19 pandemic, several outbreaks occurred in workplaces. As a result, local authorities implemented restrictive interventions (e.g., lockdown and social distancing) to control the spread of this disease in different contexts. Despite the short-term positive impacts of these interventions, they are not sustainable in the long run due to their associated economic costs to industries. Hence, in the post-pandemic era, novel and non-restrictive interventions are needed to limit the spread of similar diseases inside workplaces during epidemics. Herein, several non-restrictive interventions have been introduced to limit the spread of COVID-19 in office spaces. The effectiveness of these interventions is tested in generic office space by a disease spread simulator (CoDiSS), which is based on stochastic agent-based modeling. As a result, this research identifies the most impactful interventions based on the simulation outcomes and offers practical strategies to improve occupational safety within office environments. Our findings help enhance safety in the ever-transforming occupational environment by limiting the spread of infectious diseases in workplaces using non-restrictive interventions.

1. Introduction

The COVID-19 pandemic has raised concerns regarding the resilience of human societies against widespread infectious diseases. Several COVID-19 outbreaks proved that our urban infrastructure lacks the capacity to withstand the spread of infectious diseases, especially in those settings where people gathered within an enclosed space, such as healthcare and education infrastructure. As a result, local authorities suggested several pharmaceutical (i.e., vaccination) and non-pharmaceutical interventions (e.g., national lockdowns, social distancing, and mask mandates) to limit the spread of COVID-19 (Flaxman et al., 2020; Perra, 2021). The suggested interventions can be categorized as restrictive and non-restrictive interventions (Arena et al., 2022). Restrictive interventions refer to those implications that significantly change the personal or social behaviors of citizens. The face mask mandate and social distancing are two examples of restrictive interventions which affect citizens' personal and social behaviors, respectively. In contrast, non-restrictive interventions refer to those implications that limit the spread of COVID-19 without significantly changing their personal and social behaviors, such as increasing air ventilation rates or changing the interior design of indoor spaces. Despite the satisfactory results of the restrictive interventions in the short run (Bo et al., 2021), their implementation is not sustainable in the long run due to their high socio-economic costs (Allen, 2022; Corbaz-Kurth et al., 2022; Wali, 2023). These costs include the increased rate of adolescent psychiatric disorders during the lockdown (Guessoum et al., 2020; Pauksztat, Andrei, & Grech, 2022), the increased job insecurity (Bazzoli & Probst, 2022; Vu, Vo-Thanh, Nguyen, Van Nguyen, & Chi, 2022), and reduced GDP in several developed countries. One of the key reasons for these high socio-economic costs is the lack of engineering solutions to develop workplaces that can operate safely during epidemics (i.e., disease-resilient workplaces).

COVID-19 is a respiratory infectious disease, which is transmitted from an infected individual to a susceptible one through the airborne (aerosol), droplet, or vehicleborne (fomite) transmission routes (Khan et al., 2021). Despite the initial speculations about the dominance of the droplet transmission route, several recent studies confirmed that the dominant route of COVID-19 transmission is airborne (Jiang et al., 2021; Lewis et al., 2022; Tellier, 2022). Accordingly, the non-restrictive interventions for limiting the spread of COVID-19 in indoor spaces are limited to two engineering solutions: air ventilation and air purification (Berry, Parsons, Morgan, Rickert, & Cho, 2022). These systems reduce the concentration of viral pathogens in indoor spaces by indoor-outdoor air exchange (ventilation) or by removing viral pathogens by air filtration or disinfection (air purification) (Park, Yook, & Koo, 2022). Despite the effectiveness of these systems, their high energy

* Corresponding author.
E-mail address: nima.gerami-seresht@durham.ac.uk (N. Gerami-Seresht).

https://doi.org/10.1016/j.scs.2023.104781
Received 30 March 2023; Received in revised form 8 June 2023; Accepted 3 July 2023
Available online 13 July 2023

consumption has raised concerns among the building engineering community (Choi & Yoon, 2023). The air cooling system (air ventilation) is the most energy-demanding end-use in buildings, consuming almost 40% of the total buildings' energy consumption (González-Torres, Pérez-Lombard, Coronel, Maestre, & Yan, 2022). Consequently, after easing COVID-19 restrictions and reopening the economy, the increased rate of air ventilation systems in indoor spaces has risen by 6%, compared to the pre-pandemic time (IEA, 2022). This increase is equivalent to a 3% increase in total buildings' energy consumption (IEA, 2022). Hence, there is a research gap in analyzing COVID-19 spread at the micro level and developing novel and sustainable engineering solutions to build disease-resilient workspaces in the post-pandemic era.

The research community tackled this challenge by modeling the spread of COVID-19 by several modeling techniques, including statistical methods (Chu, 2021), computational fluid dynamics (CFD) (Che, Ding, & Li, 2022; Sheikhnejad et al., 2022), and agent-based modeling (ABM) (Kerr et al., 2021; Martinez, Bruse, Florez-Tapia, Viles, & Olaizola, 2022; Raoufi & Fayek, 2021). In these efforts, scholars often concentrated on modeling the spread of COVID-19 in different settings, ranging from the country- or state-wide spread of the disease (Katal, Wang, & Albettar, 2022; Krivorotko, Sosnovskaia, Vashchenko, Kerr, & Lesnic, 2022; Li & Giabbanelli, 2021) to the spread of COVID-19 in classrooms (Che et al., 2022). Considering their modeling scope, these efforts can be categorized as (I) macro-level models that simulate the spread of COVID-19 in large geographical areas, among large populations (i.e., national-, or state-level models) (Aylett-Bullock et al., 2021; Kerr et al., 2021); and (II) micro-level models that simulate the spread of the disease within a limited area, among a small number of distinguishable individuals (e.g., classroom or offices) (Araya, 2021a; Martinez et al., 2022; Seresht, 2022). All of these modeling efforts (i.e., the macro- and micro-levels models) address the prognostic analysis of COVID-19 spread by predicting the spread of this disease within human populations.

While prognostic analysis is essential, research is also required on the diagnostic analysis of COVID-19 to utilize these predictive models and diagnose the main causes of disease transmission in different settings (van Smeden, Reitsma, Riley, Collins, & Moons, 2021). The diagnostic analysis, as described, helps to develop innovative, effective, and sustainable interventions for this disease in the long run. There are very few studies in the literature focusing on the diagnostic analysis of COVID-19. Additionally, those few studies that tackled the diagnostic analysis of COVID-19 concentrate on the macro-level spread of the disease and often evaluated the effectiveness of vaccination at the national, state, or city levels (Katal et al., 2022; Krivorotko et al., 2022; Li & Giabbanelli, 2021).

Diagnostic analysis of COVID-19 at the micro-level is complex since it requires considering the physical (e.g., architecture) and functional (e.g., ventilation rate) characteristics of the building, as well as the occupants' social and personal behavior (Martinez et al., 2022; Zhao, Liu, Yin, Zhang, & Chen, 2022). Incorporating buildings' physical and functional characteristics is a straightforward practice because these characteristics are static (do not change over time); however, modeling occupants' behavior poses a challenge due to its interactive and dynamic nature, as well as its dependency on several personal and social characteristics of occupants (Araya, 2021a; Seresht, 2022). Herein, a general-purpose simulation framework (contagious disease spread simulator, called CoDiSS (Gerami-Seresht & Sadeghi, 2023)) is used for prognostic and diagnostic analysis of COVID-19 spread at the micro-level. CoDiSS is an open-source simulation framework developed by the authors based on stochastic ABM. The application of ABM in CoDiSS helps capture the interactive and dynamic behaviors of occupants, as well as their interactions with the building and one another. The contributions of this paper are threefold: (I) on the prognostic analysis aspect, this paper introduces a highly granular micro-level simulation framework that captures several parameters that affect the airborne transmission of infectious diseases in indoor spaces; (II) on the diagnostic analysis aspect, this paper identifies the high-risk zones for COVID-19 transmission in office spaces; and (III) to enhance the occupational safety, this paper suggests non-restrictive interventions to limit the spread of COVID-19 in the identified high-risk zones and assesses the effectiveness of the suggested interventions through simulation.

The remainder of this paper is organized as follows: Section 2 provides a brief review of the literature on ABM and the simulation of COVID-19 spread at the macro and micro levels. Section 3 illustrates our research methodology by interpreting the spatial (i.e., related to space) and temporal (i.e., related to time) structure of CoDiSS (Gerami-Seresht & Sadeghi, 2023). Section 4 tests the validity of the research methodology by simulating the COVID-19 outbreak in a case study project and comparing the results to empirical data. Section 5 describes the research methodology for developing non-restrictive interventions and then assesses several interventions for limiting the spread of COVID-19 in office spaces. In Section 6, the results are discussed, and a strategy (combination of several interventions) to enhance occupational safety in office spaces. Finally, Section 7 presents the conclusions and discusses future research areas in this context.

2. Literature review

The research community strove to address the challenges raised by the COVID-19 pandemic by modeling the spread of COVID-19 in different settings (prognostic analysis) at both the macro and micro levels. Although a wide range of modeling techniques is utilized for macro-level modeling of COVID-19 spread, the majority of micro-level models are based either on ABM (Araya, 2021a; Martinez et al., 2022; Seresht, 2022) or CFD (Che et al., 2022; Sheikhnejad et al., 2022). The application of ABM at the micro-level is beneficial when dynamic human behavior is the main contributor to the disease spread, and CFD is useful for modeling the movements of aerosols within indoor spaces. ABM is a simulation technique with proven capability for modeling complex systems, in which the overall system performance is created by several interactions among individual components (i.e., agents) of the system (Borshchev, 2013). The following two sub-sections review the prominent efforts for modeling COVID-19 spread at the macro and micro levels and identify the research gaps in the prognostic and diagnostic analysis of COVID-19.

2.1. Macro-level modeling of COVID-19 spread

At the macro level, COVID-19 outbreaks are simulated at the city, state, or even country levels, using a range of modeling techniques, including statistical modeling (Chu, 2021), Monte Carlo simulation (Afshar-Nadjafi & Niaki, 2021; Xie, 2020), and ABM (Kerr et al., 2021; Truszkowska et al., 2021). The large modeling scale of the macro-level ABM models is associated with high computational costs and low granularity. Consequently, these models often simulate a large population of citizens by a single agent to help with their large modeling scale, simulating the behaviors of thousands or even millions of citizens. This indicates that macro-level models cannot closely trace the interactions between specific individuals in the simulation environment since they require simplification and generalization of human behaviors (Truszkowska et al., 2021). Given these characteristics, the macro-level models of COVID-19 are inappropriate for simulating the spread of this disease (i.e., prognostic analysis) in small enclosed spaces, like office spaces. This limitation can be addressed by implementing micro-level modeling of COVID-19 spread, in which the high granularity of the model allows accounting for different socio-personal behaviors of individuals within the simulation environment.

In addition to their application for prognostic analysis, the macro-level models of COVID-19 are utilized for analyzing the effectiveness of some interventions on a large scale. Jadidi et al. (2021) numerically analyzed the effectiveness of partial COVID-19 vaccination, where vaccines are not available or appropriate for all citizens. Li and Giabbanelli (2021) used Covasim (Kerr et al., 2021), a well-established macro-level simulator of COVID-19, to evaluate the effectiveness of vaccines at the national level in the United States. Their results confirm the high effectiveness of vaccines in limiting the spread of COVID-19. Similar studies in the UK (Panovska-Griffiths et al., 2022), Germany (Krebs, von Jouanne-Diedrich, & Moeckel, 2021), and Poland Latkowski and Dunin-Keplicz (2021) confirm the effectiveness of vaccination in limiting the spread of COVID-19 at the national level. In another macro-level analysis, Shorfuzzaman, Hossain, and Alhamid (2021) suggested the use of computer vision algorithms for monitoring the compliance of citizens to the social distancing mandate. Despite the usefulness of these results, these studies fail to develop and test innovative non-restrictive interventions for limiting the spread of this disease due to their low granularity. Identifying the high-risk zones for disease transmission and testing the effectiveness of new interventions (i.e., diagnostic analysis) can be accomplished by either empirical studies (Mendez-Brito, El Bcheraoui, & Pozo-Martin, 2021) or by micro-level modeling, in the latter of which all affecting parameters are sufficiently addressed.

2.2. Micro-level modeling of COVID-19 spread

The micro-level models of COVID-19 can address the physical and functional characteristics of the environment, as well as the socio-personal behaviors of its occupants, due to their smaller modeling scope (Araya, 2021a; Liao et al., 2022). This high level of granularity is associated with a significant increase in their computational costs and modeling complexity; hence micro-level models are only applicable to small areas and a limited number of individuals. A discussion by Saeedi (2018) illustrates the trade-off between the modeling scope and granularity. There are very few studies tackling the prognostic analysis of COVID-19 at the micro level due to the complexities associated with modeling buildings' characteristics and their occupants' behaviors. A few studies attempted micro-level modeling of COVID-19 spread among construction workers (Araya, 2021a, 2021b; Seresht, 2022); however, these studies fail to capture the essential parameters that affect COVID-19 transmission, such as airborne transmission, contacts, and architecture of the simulation environment. In a more recent and more comprehensive effort, Martinez et al. (2022) introduced a micro-level model of COVID-19 (ArchABM), which has a high granularity by accounting for the physical characteristics of the indoor space and modeling each individual by an agent. ArchABM is a modular framework with high scalability, and its simulation results prove the usefulness of micro-level models for the prognostic analysis of COVID-19. However, ArchABM (Martinez et al., 2022) utilizes a discrete event time engine, which limits the capability of this framework for modeling highly dynamic human behaviors and air movements inside indoor spaces since these dynamic variables can only be modeled by the continuous time engine (Bandyopadhyay & Bhattacharya, 2014). Furthermore, some critical aspects of modeling COVID-19 spread are overlooked in ArchABM, such as the changes in the viral load of the virus throughout the infection duration and the infection risk calculated based on the virus quanta inhaled. There remains a significant research gap in the prognostic analysis of COVID-19 transmission within indoor spaces, encompassing all various parameters that influence the spread of this disease.

In addition to the limitations that exist in the prognostic analysis of COVID-19 at the micro level, the diagnostic analysis of this disease is also lacking, since it is only addressed by CFD (Che et al., 2022; Sheikhnejad et al., 2022). The application of CFD for diagnostic analysis of COVID-19 completely ignores the dynamic socio-personal behaviors of occupants and concentrates on the air movements within the indoor space. Accordingly, further efforts are required to utilize the existing micro-level ABM models to simulate the disease spread in different scenarios and identify the high-risk zones of disease transmission. The high granularity of micro-level ABM models can also help to test new interventions for limiting the spread.

The following three research gaps are identified within the existing body of knowledge: (I) simulating the spread of COVID-19 in indoor spaces by a highly granular micro-level model (prognostic analysis); (II) identifying the high-risk zones of COVID-19 transmission (diagnostic analysis); and (III) developing innovative and non-restrictive interventions to limit the spread of the disease in the identified high-risk zones. These research gaps are addressed in this paper by modeling the spread of COVID-19 in office spaces using a highly granular micro-level framework, CoDiSS (Gerami-Seresht & Sadeghi, 2023), identifying the high-risk zones, and testing several non-restrictive interventions to limit the disease spread in these settings.

3. Research methodology

This section discusses the methodology for simulating COVID-19 spread in office spaces by CoDiSS. The spatial and temporal structure of CoDiSS is presented in Fig. 1, illustrating the data flow between the different modules of the framework. In every simulation timestep, CoDiSS starts with simulating the social and then personal behaviors of the agents to determine each agent's actions throughout the timestep. In CoDiSS, agent behaviors are stochastically defined by probabilistic distributions. Hence, despite all agents following the same behavioral rules, their actions are different at each time step. The stochastic behavioral rules allow CoDiSS to deliver more realistic results by simulating agents' diversity and accounting for differences in their personal attributes.

In every simulation timestep, the virus spread by infected agents is calculated based on their actions and the location within the simulation environment. Afterward, CoDiSS simulates the virus decay and the airflow within the simulation environment, and finally maps the virus concentration throughout the environment and stochastically determines the new cases of COVID-19.

Furthermore, the structure of CoDiSS is illustrated based on the ODD+D (i.e., overview, design concepts, details, and decision-making) protocol developed by Müller et al. (2013).

3.1. Overview

The objective of CoDiSS is to determine infection risks in an indoor space – an office space, in this research – while considering the physical and functional characteristics of the building and its occupants' behavior. For airborne transmission, this risk is quantitatively determined based on the Riley, Murphy, and Riley (1978) equation, considering the virus quanta that each agent inhales during the simulation run. One quantum is equal to the dose of viral pathogens required to cause infection in 63% of susceptible individuals (Buonanno, Stabile, & Morawska, 2020). In CoDiSS, each person inside the office space is modeled by an agent, and the time steps are selected by the modeler. The state variables of CoDiSS are (I) the concentration of viral pathogens inside the office space mapped over the entire space (calculated for each $1.5\ \text{m} \times 1.5\ \text{m}$ cell) and (II) the state of each agent specified by its location, task, infection state (for infected ones), and infection risk (for healthy ones).

CoDiSS is a general-purpose ABM framework for modeling the spread of infectious diseases; hence, it allows modelers to select the cell size based on the modeling context and limitations. In this research, the cell size is set to $1.5\ \text{m} \times 1.5\ \text{m}$, so that agents' walking speed is simply modeled as one cell per second, resulting in an average walking speed of $\approx 5\ (\text{km/h})$ as suggested by the literature for average women and men (Dempsey et al., 2022). Additionally, selecting the cell sizes of $1.5\ \text{m}$ allows tracking the droplet transmission of contagious diseases (in future research) since the distance between two agents within a given cell will be less or equal to $\approx 2\ \text{m}$, which is the minimum safe distance between a susceptible and infected individual for droplet transmission

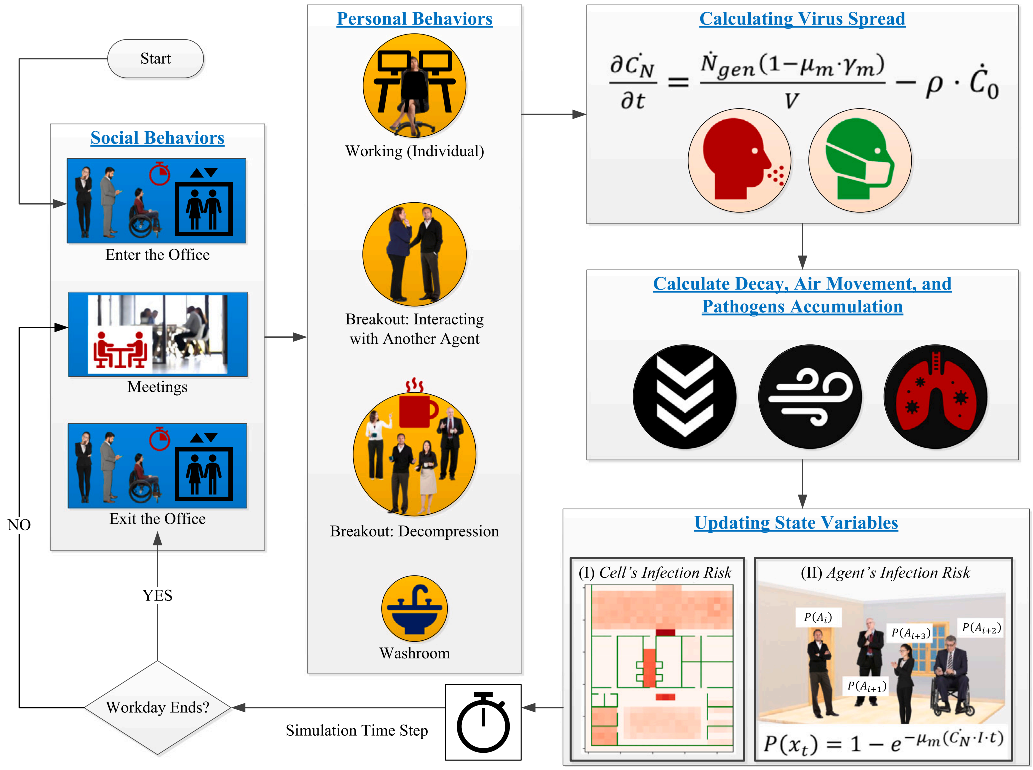

Fig. 1. The spatial and temporal structure of CoDiSS.

(i.e., maximum travel distance of large droplet nuclei before gravitational settling) (Lewis et al., 2022). The simulation process starts with creating the office layout in CoDiSS manually, creating several agents, and then simulating agents' interactions with the space and one another in continuous time progressions. CoDiSS utilizes continuous simulation time steps equal to one minute of the real-world time progression.

3.2. Design concepts

The theoretical aspect of COVID-19 transmission and the infection risks associated with different social behaviors has been comprehensively discussed in epidemiology literature (Fang, Karakiulakis, & Roth, 2020; Lancet, 2020). Generally, infectious diseases may be transmitted from an infected individual to a susceptible one through one of the following transmission routes (Dicker, Coronado, Koo, & Parrish, 2012):

- Direct Transmission
  - Direct Contact: Direct transmission occurs if the infectious agents (e.g., bacteria, viral pathogens) are transmitted through skin-to-skin contact between two individuals.
  - Droplet Spread: Droplet spread occurs through the short-range spray of large droplets (>5 μm) created by an infected agent through sneezing, coughing, or normal breathing.
- Indirect Transmission
  - Airborne Transmission: Airborne transmission (also called aerosol transmission) occurs by the small repository droplets or droplet nuclei, which are smaller than 5 μm in diameter and may float in the air for extended periods until the pathogens are deactivated (i.e., viral decay) or removed from the air either by gravitational settling, ventilation or air purification.
  - Vehicleborne Transmission: Vehicleborne transmission occurs when infectious agents are transmitted to susceptible individuals through a contaminated vehicle that has been in contact with an infected individual earlier. These vehicles can be food or water, biological products (e.g., blood), or fomites (e.g., bedding or objects' surfaces). Hence, this transmission route is also known as fomite transmission.
  - Vectorborne Transmission: In this transmission route, the infectious agents are transmitted from an infected individual to the susceptible one through insects' vectors (e.g., mosquitoes, fleas). These insects may be just a mechanical career of the viral pathogens or support the growth and change of the infectious agent.

Despite the initial speculations (Jimenez et al., 2022), recent studies confirm that airborne (aerosol) transmission is the dominant transmission route of COVID-19 (Jiang et al., 2021; Tellier, 2022). Thus, CoDiSS only simulates the airborne transmission of COVID-19 in office spaces in this research. At each simulation timestep, it identifies the infected individuals inside the office space and calculates $\dot{NE}_{i,j}$, denoting the number of pathogens exhaled by all infected agents at the (i,j) coordinate. The number of pathogens exhaled by an agent is determined based on the activity it undertakes in each simulation time step, using the experimental data provided in the literature (Goyal, Reeves, Cardozo-Ojeda, Schiffer, & Mayer, 2021; Lancet, 2020; Liu et al., 2020). In this research, agents either sit, talk, or walk within the office space, and the number of pathogens they exhale is determined accordingly. Next, in each simulation time step, CoDiSS calculates the changes in the concentration of viral pathogens inside the office, as presented in Eq. (1). The notation of $\dot{C}^t_{(i,j)}$ represents the concentration of pathogens in the specific cell denoted by (i,j) at time t. Here, the indexes i and j are the cell's row and column number, respectively. In its default settings, CoDiSS sets the concentration of viral pathogens equal to zero at the start of every day (as well as simulation start), where weekdays are tracked by the built-in calendar in CoDiSS.

$$\frac{d\dot{C}_{i,j}}{dt} = \frac{\dot{NE}_{i,j}(1-\mu_m \cdot \gamma_m)}{V} - \rho \cdot \dot{C}^t_{i,j} \tag{1}$$

where the differential $d\dot{C}_{i,j}$ denotes changes in the concentration of pathogens in cell (i,j), dt stands for the simulation time step; μ_m is for

Table 1
The probability, duration, and location of the tasks assigned to each agent.

Task	Probability/Duration	Location	Social or personal
Enter\Exit	3 min	Elevator or entrance	Social
Meeting	60 min	Meeting rooms	Social
Decompression	Uniform [3–6%]	Coffee spot	Personal
Working	Uniform [86–93%]	Assigned desk location	Personal
Interaction with another agent	Uniform [3–6%]	Other agent's desk	Personal
Washrooms	Uniform [1–2%]	Washrooms	Personal

the efficiency of masks used by the occupants (i.e., $\mu = 0$ if no masks are used); γ_m is the rate of occupants' compliance with the mask mandate. Additionally, V represents the total volume of the confined space (i.e., equal to 6.75 m^2 for a cell of 1.5 m wide and 3 m tall in this research), and ρ denotes the decay rate of the viral pathogens. The decay rate covers gravitational settling (i.e., the number of droplets settled due to the gravitational force), viral deactivation— calculated based on the details provided in epidemiology literature (Lancet, 2020) — as well as the removal rate by air ventilation and air purification systems. CoDiSS also accounts for changes that occur in different disease stages (e.g., non-symptomatic non-contiguous, non-symptomatic contiguous) in terms of viral pathogens released by infected individuals (Liu et al., 2020).

Air movement inside an enclosed space is a major contributing factor to the aerosol transmission of infectious diseases. There are several features that affect air movements inside an enclosed space (e.g., architecture, ventilation, and occupancy), which can be modeled by advanced CFD methods. For the sake of modeling simplicity, CoDiSS only accounts for the space architecture and average ventilation rate while modeling air movement inside the simulation environment. In a simple CFD formulation presented in Eq. (2), CoDiSS calculates the speed of air movements – equally distributed in four main directions – based on the average ventilation rate inside the enclosed space (Bhagat, Wykes, Dalziel, & Linden, 2020).

$$S = 0.8v\ (\mathrm{mm/s}) = 4.8v \cdot 10^{-2}\ (\mathrm{m/min}) \tag{2}$$

where S denotes the speed of air movements, and v stands for the average ventilation rate. CoDiSS also accounts for space architecture by only allowing air movements through open spaces and blocking air movements through walls and doors. Further details regarding CoDiSS can be found in the documentation of the open-access Python library published by the authors (Gerami-Seresht & Sadeghi, 2023).

Agents' decision-making is based on their social and personal behavior, where the former is an attribute of the simulation environment and applies to all agents. The latter is a personal attribute and may vary from one agent to another. In CoDiSS, agent behaviors are determined based on stochastic behavioral rules defined by probability distributions. Such stochastic behaviors provide a realistic representation of real-world scenarios. Instead of imposing deterministic behaviors, the model incorporates random occurrences of common behaviors and allows for the emergence of diverse patterns with varying durations. For example, on every meeting occurrence, the attending agents are randomly selected. This probabilistic approach reflects the unpredictability and variability often observed in the actual office settings.

Two aspects of social behavior are considered in this framework: (I) the work schedule that determines the timing of entering and exiting the office space; and (II) meeting with several agents in the allocated meeting rooms. The personal behaviors of agents involve: (I) working at the desk allocated to the agent; (II) taking a rest break at the decompression area (e.g., tea or coffee break); (III) taking a rest break and interacting with another agent (a colleague); and (IV) using washrooms. At each simulation timestep, each agent is assigned to one of these tasks based on the transition probabilities given in Table 1, considering that the social behaviors override the personal ones. For example, if an agent is assigned to a meeting (i.e., a social behavior), it will attend the meeting regardless of its personal behavior assignment (e.g., working at its desk). Tasks undertaken by agents and their corresponding probabilities and locations are presented in Table 1.

The probabilities and durations of tasks, shown in Table 1, are extracted from multiple resources in the literature (Afacan & Gurel, 2015; Blasche, Pasalic, Bauböck, Haluza, & Schoberberger, 2017; Verizon, 2003), which focused on quantifying office work allocations. According to the literature, an average office worker takes 2.9 rest breaks, each last between [9.3–20.2 min] (Blasche et al., 2017). The duration of time spent in the rest breaks is equally distributed between "Interaction with Another Agent" and "Decompression" in Table 1. The literature also suggests the daily time allocation for using washrooms for a healthy individual is [9–20 min]. Finally, in this paper, the ABM framework simulates meetings are simulated by creating four meeting events per day and randomly selecting their participants from all present agents. The transitional probabilities that define the personal behavior of the agents are calculated as uniform distributions based on these tasks' durations (see Table 1).

Once all agents are assigned to given tasks at each simulation time step, the concentration of viral pathogens (state variable 1) is updated, and the infection probability is determined for each healthy agent (state variable 2) inside the office. The ABM framework determines the infection probability based on the Wells-Riley equation (Riley et al., 1978) presented in Eq. (3) (de Oliveira, Mesquita, Gkantonas, Giusti, & Mastorakos, 2021; Watanabe, Bartrand, Weir, Omura, & Haas, 2010).

$$P_x(t) = 1 - \exp\left(-N\dot{I}_x(t)\right) \tag{3}$$

where $P_x(t)$ stands for the probability of agent x getting infected at time t, and $N\dot{I}_x(t)$ is the total quanta of pathogens inhaled by agent x until the simulation time t. The total quanta inhaled by agent x (represented as $N\dot{I}^x(t)$), who stays in the cell (i, j) for the duration of t is calculated by Eq. (4).

$$N\dot{I}_x(t) = \int_{t_0}^{t} (1 - \mu_m \gamma_m) I_x \dot{C}^t_{i,j} \cdot dt \tag{4}$$

where $\dot{C}^t_{i,j}$ denotes the concentration of viral pathogens in the cell (i, j) at time t (See Eq. (1)). Additionally, I_x represents the air inhalation rate of the agent, determined based on its activity at each simulation time step using the details provided in epidemiology literature (Lancet, 2020). Furthermore, dt stands for the duration of the simulation timestep (i.e., 1 min), and μ_m and γ_m denote mask efficiency and compliance, respectively. The compliance with mask usage is quantified as the percentage of time during which agents consistently wear masks over their face. Given Eqs. (3) and (4), the contribution of each cell to the infection risk of all healthy agents – hereafter referred to as the cell infection risk ($CIR_{i,j}$) – can be calculated as shown in Eq. (5).

$$CIR_{i,j} = 1 - \exp\left(-\sum_{x=0}^{NH} N\dot{I}_x(t_{\max})\right) \tag{5}$$

where NH indicates the total number of healthy individuals in the office, and $t_{\max}$ denotes the total simulation runtime. The cell infection risk, as defined in Eq. (5), indicates the probability of any healthy agent getting infected in the given cell throughout the simulation run. In this research, the cell infection risk (CIR) is used to determine the high-risk zones of COVID-19 transmission in office spaces and to evaluate the effectiveness of non-restrictive interventions in limiting the spread of COVID-19 in office spaces. According to the cell infection risk formulation (Eq. (5)), the two following conditions are required for a given cell to become a high-risk zone of COVID-19 transmission: (I) having a high concentration of virus quanta throughout the simulation run; and (II) having a high footfall of healthy agents.

3.3. Implementation details

CoDiSS is an open-source Python library, which is developed with a modular architecture and is available on GitHub (Gerami-Seresht & Sadeghi, 2023) for non-commercial applications. On simulation initialization, the simulation environment is created by mirroring the physical characteristics of the office space. To this end, CoDiSS creates a network of 1.5 m-wide cells over the entire office layout based on the coordinates of the layout boundaries given by the modeler. Next, the modeler manually defines the boundaries of each cell as an open space or wall. Once the simulation environment is created, several agents are created and enter the building (i.e., office) from the designated entrance and move to their designated working space (i.e., desk). Then, agents' behavior is re-created in CoDiSS by randomly assigning each agent to one of the tasks – manually defined by the modeler – at each simulation time step. Since the ABM framework used in this article is a general-purpose framework for simulating the spread of contagious diseases (not specific to COVID-19 nor office spaces), the disease specifications and tasks undertaken by each agent are manually defined and empirically validated (see Section 4).

3.4. Decision-making on appropriate non-restrictive interventions

First, the cell infection risk CIR_I is mapped inside the office by CoDiSS, and areas with the highest CIR_I – hereafter called high-risk zones – are identified. Next, several non-restrictive interventions are suggested to reduce the infection risk in these high-risk zones. Non-restrictive interventions refer to any intervention that limits the spread of COVID-19 without significantly changing the work behavior of employees (like social distancing) or requiring compliance of individuals (like face masks and vaccination). Notably, the non-restrictive interventions we suggest in this research may involve minor or major spatial changes to the office space; however, it aims to minimize the impacts on the temporal structure of the system (i.e., employees' behavior) or the business capacity at the given office space.

Decision-making regarding the most effective non-restrictive interventions is made based on two performance indicators: (I) the number of agents infected during the simulation over the total number of agents (hereafter called infection rate); and (II) the cell infection risk (CIR), averaged over the entire office space (see Eq. (5). Given the stochastic behavior of the spread of infectious diseases, these performance indicators are calculated for each intervention for 100 simulation runs – using Monte Carlo simulation – and the average results are reported.

For the sake of comparison, the spread of COVID-19 in the original settings of the case study office (hereafter called base scenario) is simulated, and the two performance indicators are calculated for the base scenario. Next, by implementing each non-restrictive intervention, its performance indicators are compared to the base scenario (infection rates and CIR). Furthermore, the statistical significance of the difference between the base scenario and implemented interventions is evaluated using the t-tests. For two random distributions (e.g., infection rates in the base scenario and the post-intervention scenario) with the averages of m_1 and m_2, the t-test is applied by calculating the t using Eq. (6).

$$t = \frac{m_1 - m_2}{\sigma_d \sqrt{\frac{1}{n_1} + \frac{1}{n_2}}} \tag{6}$$

where σ_d represents the standard deviation of the differences between the two samples, and n_1 and n_2 are the sample sizes of the first and second distributions, respectively. The t values are then compared to the critical t-value at 95% confidence level, and the statistical significance of each intervention's impact is statistically tested.

Additionally, the cost of implementing each intervention is incorporated into the decision-making process by assessing the implementation costs. While a comprehensive cost analysis could incorporate factors such as the actual financial cost and adherence difficulty, our research focuses specifically on assessing the effectiveness of interventions rather than conducting a detailed cost evaluation. Therefore, a three-point Likert scale (i.e., low, $medium$, and $high$) is used based on the authors' subjective judgment.

3.5. Developing a strategy to improve occupational safety

Once all suggested interventions are tested, we propose an additive approach to combine multiple interventions one step at a time and develop a strategy to improve occupational safety in office spaces. To this end, we start with the low-cost interventions with the highest effectiveness – based on the t-test results – in limiting the spread of COVID-19. After implementing each intervention, the spread of COVID-19 in the office space is simulated, and the new high-risk zones are identified. Consequently, the next intervention is selected based on the updated high-risk zones. In other words, the selection of non-restrictive interventions for this strategy is based on the following three criteria:

- Interventions significantly (i.e., statistical significance) reduce the infection rate (i.e., efficiency).
- Each intervention targets a distinct (different from other interventions) high-risk zone to reduce its CIR.
- The implementation cost of interventions is either low or $medium$.

In each evolution, a new intervention is selected based on the above-mentioned criteria and added to the developing strategy. Upon implementing each intervention, the cell infection risk CIR is calculated for the entire office, and the statistical significance of the evolution is tested by the t-test method at 95% confidence level. This process continues until all interventions are considered. Finally, the last evolution represents our proposed strategy for improving occupational safety in office spaces in the post-pandemic era.

4. Model validation

In this section, the research methodology and accuracy of CoDiSS are validated by simulating the spread of COVID-19 in a case study of a call center in South Korea and comparing the simulation results to the empirical data. For this purpose, we will simulate the spread of COVID-19 in the case study, where the spatial and temporal structure of the office is determined based on the information provided by Park et al. (2020) and the literature. Next, we will compare simulation results for the daily number of infections over – averaged over 100 simulation runs – to the empirical data (Park et al., 2020) to determine the accuracy of CoDiSS in predicting the COVID-19 infection rate in the case study. We will also apply the behavior reproduction test at extreme conditions by comparing the number of new cases reported on weekends to the empirical data (i.e., zero new cases).

The case study concerns the spread of COVID-19 in a call center, which is located on the 11th floor of a 19-story commercial building in downtown Seoul, South Korea. The outbreak was reported on March 8th, 2020, and the call center building was closed on March 9th, 2020, immediately after the report. Following its closure, all occupants were tested; consequently, all positive cases were isolated, and the negative cases were quarantined, monitored, and retested during a fourteen-days window. Among the total 1143 residents of the building, 97 positive cases of COVID-19 were reported. Notably, 97% of the positive cases (i.e., 94 cases out of the total 97 infected individuals) were working on the 11th floor of the building in the call center; hence, this case study concerns this call center only. The empirical data, including the

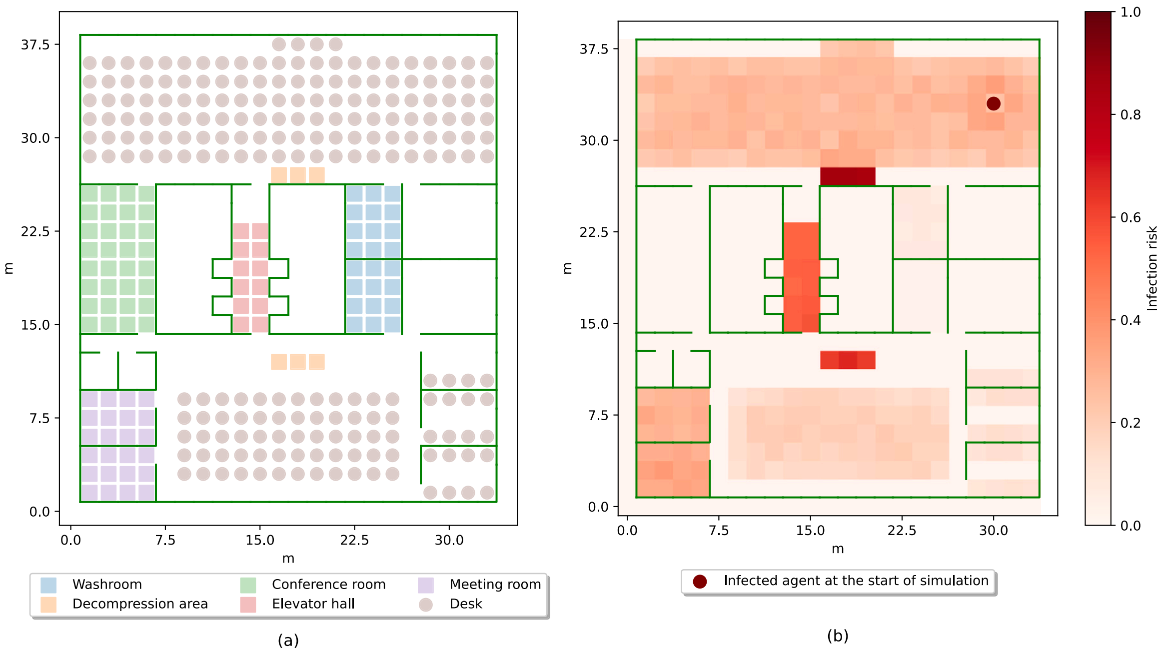

Fig. 2. The call center case study layout.

epidemiological details of the outbreak and the physical characteristics of the office space, are further discussed by Park et al. (2020).

First, the office layout is created in CoDiSS by defining the exterior and interior walls of the office space, assigning the workspace of 216 employees, and specifying the common-use locations within the office space (e.g., the decompression areas, elevators, washrooms, and meeting rooms). The office layout with all the aforementioned spatial details was presented by Park et al. (2020) and was re-created in CoDiSS, as presented in Fig. 2(a).

The office layout, presented in Fig. 2(a), comprises two primary larger working zones and several smaller zones, referred to as clusters, situated on the north and south wings of the office. Within this context, we define cluster size as the number of individuals working in the same indoor environment without any partitions or panels segregating them. The upper and lower zones are connected by the conference room and the elevators' hallway in the center. Each cluster has designated washrooms and decompression areas (also called common areas); hence employees in each cluster will only use their own cluster's common areas. In the original settings (i.e., base scenario), all employees are assumed to work in one shift for a total of 7 h [9:30 AM–4:30 PM] on Mondays-Fridays, and 5 h [9:30 AM–2:30 PM] on Saturdays (working days are similar to those reported in the case study Park et al., 2020). By implementing this work schedule, all individuals will work for 40 h per week, following the guidelines set by the South Korean employment law (Silkin, 2023). At the start of the simulation run, employees (i.e., agents) randomly arrive at the building in a 15−min window before their workday starts ([9:15 AM–9:30 AM]). Similarly, exiting the office is simulated, assuming the agents would leave the office within a 15−min window after their workday ends ([4:30 PM–4:45 PM]). Given that all employees' workday starts and finishes simultaneously, all agents will spend three minutes waiting in the hall before entering the elevator's cab. The socio-personal behavior of all employees is manually defined in CoDiSS based on the details discussed in Section 3.2.

Fig. 2(b) presents CoDiSS output for the base scenario, which maps the infection risk of each cell – calculated by Eq. (5) – on the entire office layout after completing the simulation run. Additionally, the first infected individual is specified by a red circle in Fig. 2(b) since its location can significantly affect the infection spread inside the office space. As the simulation results (i.e., diagnostic analysis) confirm, the highest risk of infection is observed in (I) decompression areas, where agents gather during the work breaks and multiple agents may interact with one another; (II) the elevators' hallway, which is densely populated at the start of the end of working hours; (III) meeting rooms due to the increased virus quanta emission rate while agents speak during meetings; and (IV) the open workspace, where agents spend the majority of their time while in the office. The simulation results also confirm that the north wing cluster has a higher risk of infection as compared to the south wing since the first case of COVID-19 was observed in the north wing cluster. The high-risk zones identified at this stage are utilized for defining the proper non-restrictive interventions in the office, as discussed in Section 5.

According to Park et al. (2020), the first symptomatic case of COVID-19 was reported on 25th of February when an employee, located on the north wing of the building – specified by a red circle in Fig. 2(b) –, developed COVID-19 symptoms. Considering an average of four days gap between the infection time and the first symptoms of the disease (Shamil, Farheen, Ibtehaz, Khan, & Rahman, 2021), the simulation of the case study starts on the 21th of January 2020. Given the stochastic nature of infectious diseases spread, the model is simulated for 100 times, and the average simulation result is compared with the empirical data, as shown in Fig. 2.

As shown in Fig. 3, CoDiSS demonstrates its effectiveness by accurately predicting the rising trend of cases over time and capturing the extreme conditions experienced during the weekend of March 1st, where the model successfully reflects no new reported infections. Additionally, the error of the simulation results (i.e., the infection rate) is calculated using Eq. (7).

$$RMSPE = \sqrt{\sum_{i=1}^{n}\left(\frac{Pr_i - Ac_i}{Ac_i}\right)^2 \frac{100}{n^2}}\% \tag{7}$$

where Pr_i and Ac_i stand for the predicted and actual values of the ith data point, respectively, and n represents the total number of data points (i.e., the number of days simulated). The results confirm that the CoDiSS predicted the cumulative number of infections with 8% error ($RMSPE$ = 8%) in this case study. Considering that the spread of infectious diseases is highly random, the prediction accuracy achieved by CoDiSS ($RMSPE$ = 8%) confirms the behavioral validity of this simulation framework.

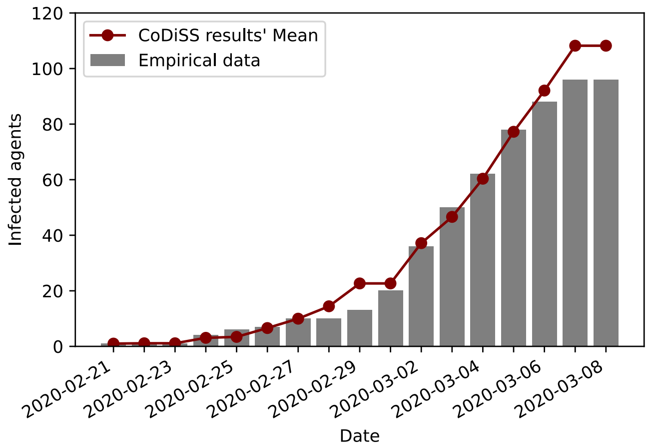

Fig. 3. Actual data and stochastic simulation results for the call center case study.

5. Non-restrictive intervention for limiting the spread of COVID-19 in office spaces

The non-restrictive interventions introduced in this paper can be grouped into two major categories: (I) the spatial interventions that alter the physical characteristics of the office space to limit the spread; and (II) the temporal interventions that make insignificant changes to individuals' work behavior. Fig. 4 provides further details regarding these two categories and the range of changes considered for each intervention.

It is noteworthy that category III represents the common interventions widely implemented by authorities during the COVID-19 pandemic, which are often deemed restrictive in certain settings and challenging to sustain in the long run. Conversely, interventions falling under Categories I and II, entailing alterations to the office layout or subtle adjustments in agents' work behavior, which demonstrate significant feasibility across diverse scenarios. With regard to office layout modifications, simple yet cost-effective measures can be implemented, such as incorporating additional panels to establish well-defined working areas or utilizing larger rooms for meetings. Furthermore, adapting work dynamics, such as reducing meeting durations or implementing minor shift changes, can be relatively straightforward to put into practice compared to more restrictive measures like mandating masks or vaccinations. These non-restrictive interventions can offer a flexible and adaptable approach to maintaining a safe work environment.

This study simulates the impact of eight interventions for limiting the spread of COVID-19 in office spaces, as presented in Fig. 4. These interventions are: (I) changing workspace settings from open workspace to clustered workspace, (II) changing the average size of clusters (III) increasing decompression space allocation, (IV) increasing meeting space allocation, (V) decreasing meetings duration, (VI) decreasing the number of meetings participants, (VII) increasing the number of working shifts (or reducing the occupancy density), and (VIII) allocating and prolonging the permissible time window to enter and exit the office.

Most interventions suggested in Fig. 4 can be implemented by simply changing the office layout or slightly changing the work behavior of the agents. The unit of measure and the range of changes for each intervention are also presented in Fig. 4. Additionally, two globally accepted restrictive COVID-19 interventions (i.e., using face masks and vaccination) are analyzed by CoDiSS, and their results are compared to our suggested non-restrictive interventions. The compliance and effectiveness of the face mask and vaccination mandates – shown in Fig. 4 – are extracted from the literature (Agency, 2023; Office of National Statistics, 2023; Sankhyan et al., 2021). To analyze the effectiveness of each intervention, the baseline values (referred to as "Base" in Fig. 4) for all spatial or temporal parameters are set based on the case study project (including the location of the initially infected agent); then, the given spatial or temporal intervention is implemented in several scenarios by gradually altering the corresponding simulation parameter. Next, the effectiveness of each intervention is determined by two performance indicators: (I) the infection rate and (II) the mapping of CIR over the office space. These two indicators are compared with the results of the case study project in its original settings (base scenario) using statistical t-test at 95% confidence level.

The mapping of CIR for the base scenario, presented in Fig. 2(b), reveals the decompression area, elevators hall, the workplace occupied by the infected agents, and the meeting rooms are the high-risk zones for transmitting COVID-19 to the healthy agents inside the office space. In the following sub-sections, the impact of different interventions on reducing the CIR and infection rates in these spaces is tested.

5.1. Work environments settings

The original setting of the case study involves two large work clusters in which the desks are located inside an open workspace. In these settings, agents can freely move and the air – and viral pathogens carried by aerosols – are distributed within the entire workspace. The distribution of viral pathogens in this settings, can increase the infection risks within the entire office space. As graphically shown in Fig. 2(b), the workplace of the infected agents is one of the high-risk zones inside the office space; hence, developing smaller work clusters and reducing the total number of employees working inside an enclosed space is expected to reduce the overall risk of infection.

To analyze the impacts of the work environment settings, the two large clusters are divided into smaller clusters by adding new wall partitions while keeping the total number of employees unchanged. Next, the average cluster size (ACS) of the employees is calculated using Eq. (8).

$$ACS = \sum_{x=1}^{N} \frac{CS_x}{N} \tag{8}$$

where CS_x is the cluster size of the xth agent and N is the total number of agents.The agents' cluster sizes vary depending on their desk location. For instance, in the base scenario, agents working in the north wing are part of a larger working cluster with a size of 136. On the other hand, agents occupying smaller offices in the south wing have a cluster size of 8. As a result, we have 136 agents belonging to a cluster of size 136. Referring to Fig. 2(b) presenting agents' working spaces, the Average Cluster Size (ACS) for the base scenario can be calculated as:

$$\frac{136^2 + 60^2 + 8^2 + 8^2 + 4^2}{216} \approx 103$$

The ACS is gradually reduced to 32.5, 19.1, 9.4, and 6.6 people by adding wall partitions in the office layout, as presented in Fig. 5. For each ACS, the simulation model ran 100 times, simulating the spread of COVID-19 in the office space between Feb. 21st and Mar. 9th, 2020. Notably, all simulation runs start with one infected agent located on the north wing cluster (see Fig. 2[b]). Fig. 5 shows how reducing ACS affects the cell infection risk (CIR) in the workplace by mapping the CIR in the entire office for different layouts. Please note that Fig. 5(a) corresponds to the base scenario, which essentially mirrors Fig. 2(b). The base scenario is included in all subsequent figures for easy comparison of the simulation results and to ensure consistency and coherence in evaluating each intervention. Additionally, according to the results presented in Fig. 6, reducing the CIR affects the daily number of infections (i.e., average infection rate).

Table 2 summarizes the simulation results and the statistical t-test on how changing the work environment settings – from open to clustered workspace – affects the spread of COVID-19 in office spaces. The t-test results indicate developing clustered workspace with average cluster sizes of 19.1, 9.4, and 6.6 can significantly (statistical

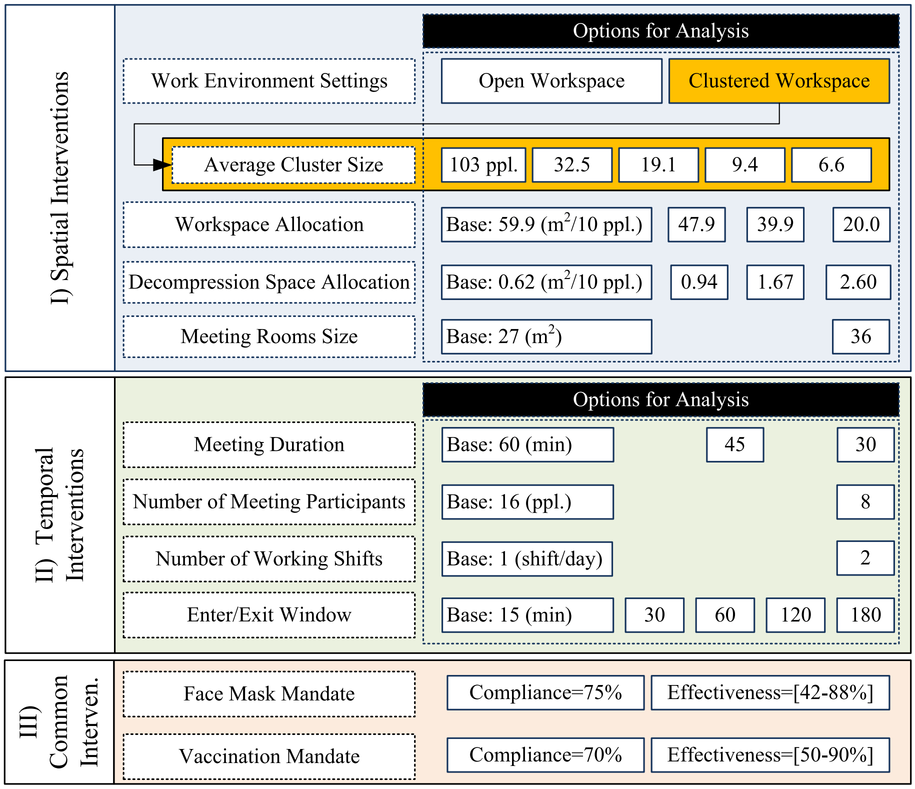

Fig. 4. Categorization of non-restrictive interventions for limiting the spread of COVID-19.

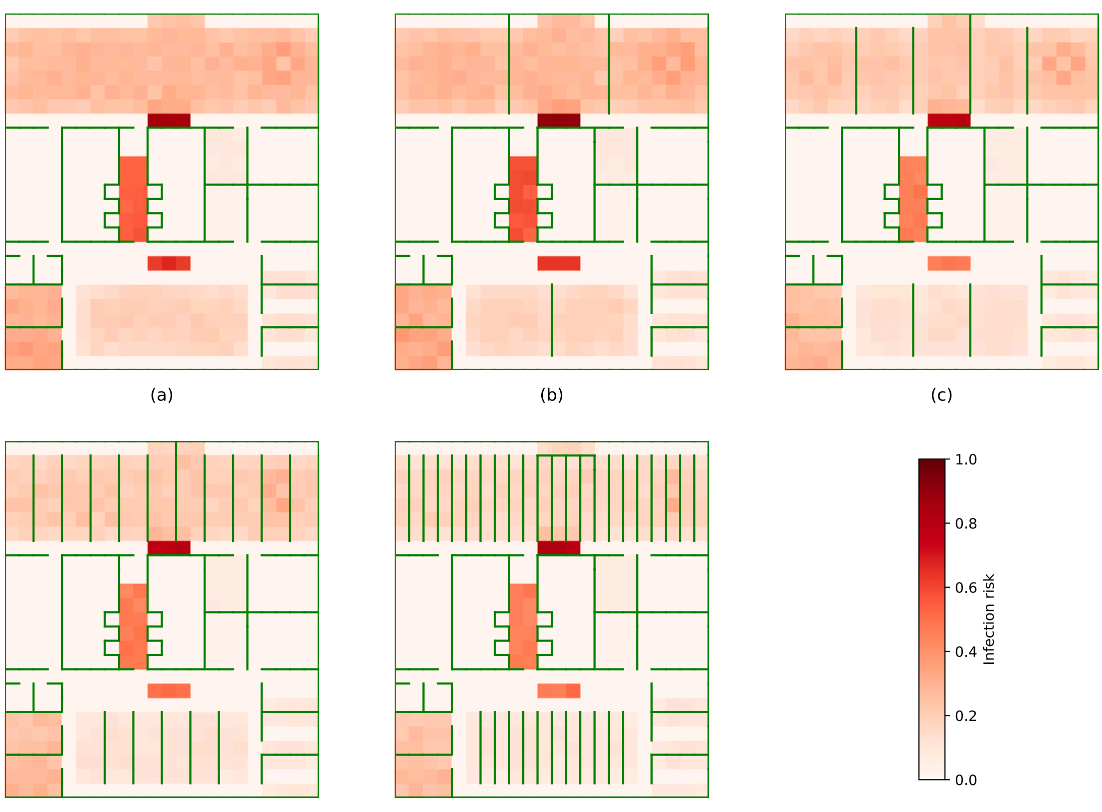

Fig. 5. The impact of reducing average cluster size on the CIR for (a) Base: 103.0, (b) 32.5, (c) 19.1, (d) 9.4, and (e) 6.6 people.

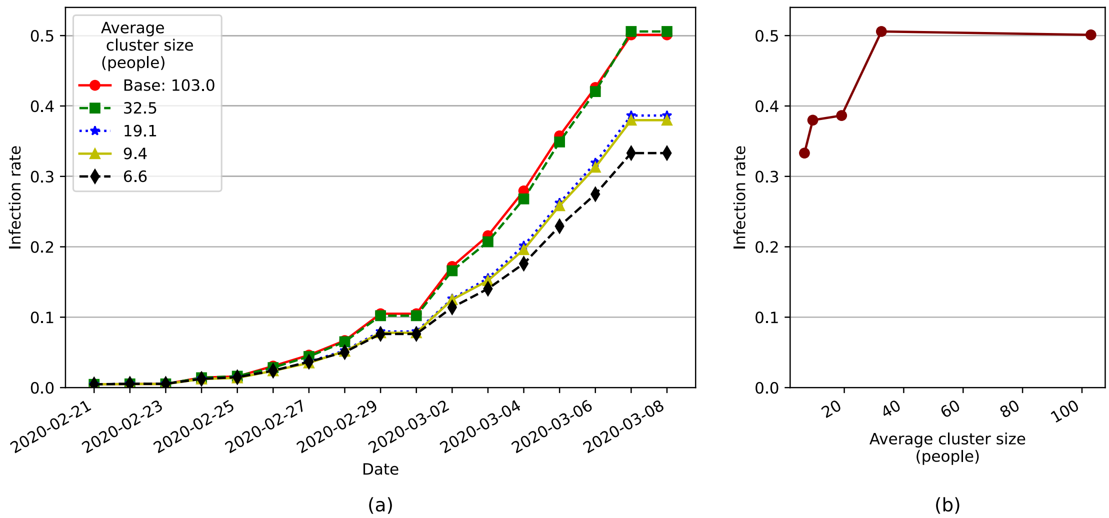

Fig. 6. (a) The impact of reducing average cluster size on the average daily infection rate, (b) Changes in the average cluster size.

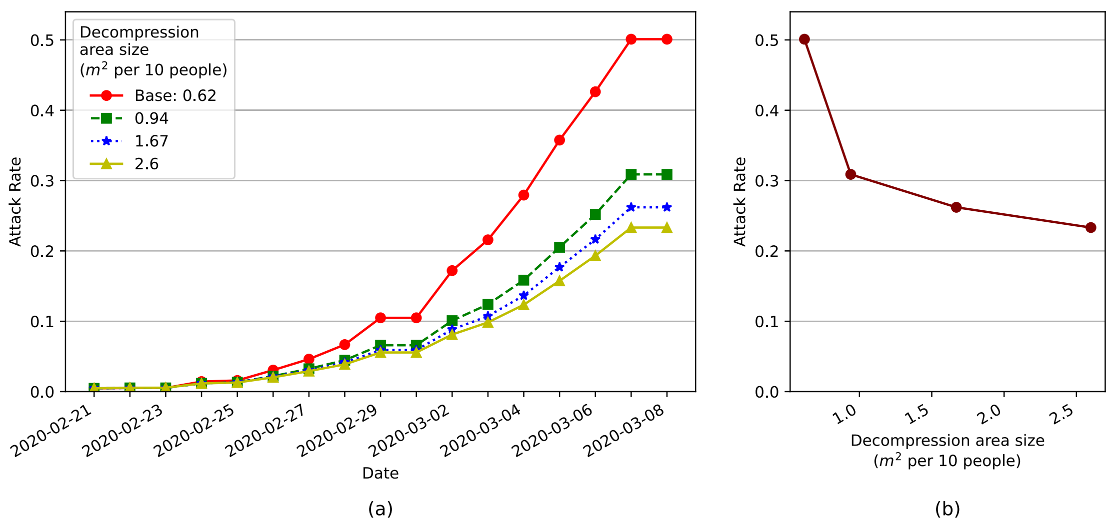

Fig. 7. The impact of decompression area allocation on the average daily infection rate.

Table 2
Summary of simulation results for reducing the average cluster size.

ACS (People)	Avg. CIR	Avg. infection rate	t-value	Statistical significance
Base: 103.0	0.112	50.1%	0.000	
32.5	0.112	50.6%	0.127	No
19.1	0.088	38.6%	−2.878	Yes
9.4	0.085	38.0%	−3.172	Yes
6.6	0.071	33.3%	−4.616	Yes

significance) reduce the COVID-19 infection rate. However, developing work clusters with an average size of $ACS = 32.5$ does not reduce the infection rate significantly.

Adjusting the office layout to reduce the ACS from 103 to 6.6 can reduce the infection rate by 17.3% (from 50.6% in the base scenario to 33.3%). Hence, simulation results suggest that developing work clusters of reasonably small sizes can enhance the resilience of office spaces against the spread of COVID-19. This is achieved by containing the viral pathogens within given clusters of the infected individuals and reducing the inter-cluster spread of the disease. The implementation cost of this intervention is rated as *low* since it can be accomplished by dividing the open workspace into several clusters using temporary or permanent wall panels without reducing the total capacity of the workspace (i.e., employees count) or affecting employees' work behavior.

5.2. Decompression space allocation

According to the simulation results presented in Fig. 2(b), decompression areas have the highest CIR in the office space. This intervention aims to reduce infection risks in these areas by increasing the total space dedicated to this purpose and avoiding high population density in decompression areas. In the base scenario, $0.62\,\mathrm{m}^2$ of decompression area is allocated to every 10 office employee. This allocation is gradually increased to $0.94\ \mathrm{m}^2$, 1.672, and $2.6\ \mathrm{m}^2$ per 10 employees, and the average infection rate and the CIR for the entire office space is predicted for each scenario through 100 simulation runs, and the results are presented in Figs. 7 and 8, respectively.

According to the presented results, increasing the decompression areas can significantly limit the spread of COVID-19 in office spaces. The simulation results reveal that increasing the decompression area by $2\ \mathrm{m}^2$ per 10 employees can reduce the average infection rate by 26.8%. Considering the small initial allocation to the decompression areas in the base scenario ($0.62\ \mathrm{m}^2/10$ ppl.), such an increase in this allocation is feasible within the given layout without compromising

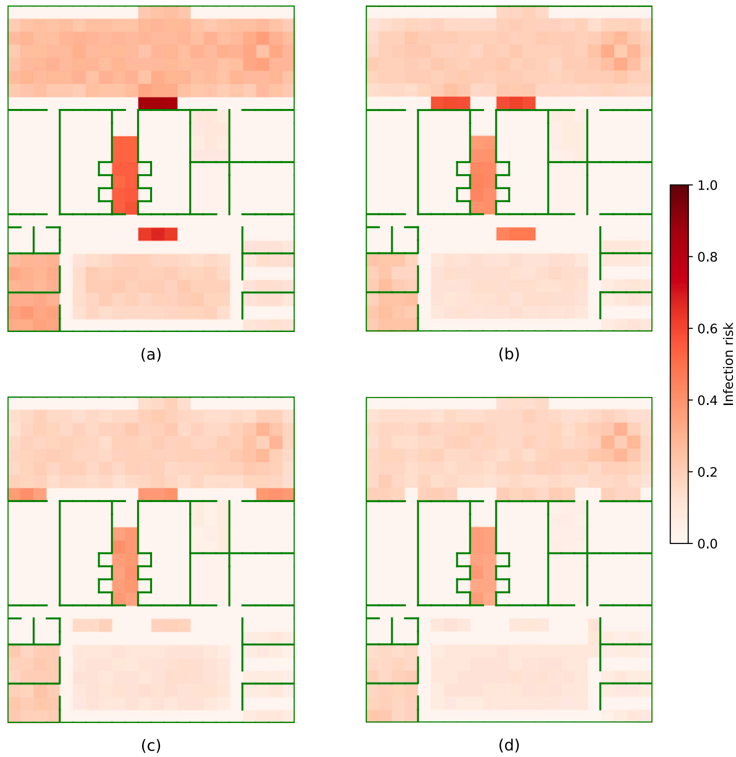

Fig. 8. The impact of decompression area allocation on CIR for (a) Base: 0.62, (b) 0.94, (c) 1.67, and (d) 2.6 (m^2 per 10 people).

Table 3
Summary of simulation results for increasing the size of decompression area.

Decompression area size (m^2 per 10 people)	CIR	Avg. infection rate	t-value	Statistical significance
Base: 0.62	0.112	50.1%	0.000	
0.94	0.082	30.9%	−5.122	Yes
1.67	0.073	26.2%	−6.567	Yes
2.60	0.066	23.3%	−7.550	Yes

on the workspace or re-purposing other functional spaces (e.g., meeting rooms). In other words, the allocation of decompression areas is increased by re-purposing the common areas. In other scenarios, increasing the decompression area allocation to 0.94 and $1.67\,\mathrm{m}^2/10\mathrm{ppl}$. reduced the average infection rate by 19.2% and 23.9%, respectively. Additionally, the t-test results also confirm the statistical significance of the impact of this intervention in all three scenarios, as presented in Table 3.

Increasing the decompression area allocation is rated as a *medium*-cost intervention since re-purposing common areas into decompression areas can consume the space allocated to other activities, hence, making some unforeseen changes to the work behavior of the employees. Additionally, increasing the decompression area allocation is associated with some financial costs to accommodate layout changes and purchasing furniture and equipment.

5.3. Meetings interventions

As shown in Fig. 2(b), meeting rooms are identified as one of the high-risk zones in the base scenario. To reduce the infection risk in meeting rooms, four meeting interventions (MI) are introduced and evaluated in this case study in separate scenarios. The average infection rate and the CIR mapping are calculated for each scenario through 100 simulation runs.

In the first intervention (MI1), the larger conference rooms (see Fig. 2[a]) to the meetings; hence, the meeting room size is increased from 27 to $36\,\mathrm{m}^2$. Notably, other meeting parameters (i.e., duration and the number of participants) are similar to the base scenario (60 min and 16 people, respectively). Fig. 9(b) confirms the implementation of this intervention, where the CIR is increased in conference rooms and decreased to zero in meeting rooms. In the second intervention (MI2), the number of meeting participants is changed from 16 people to 8 people to reduce the density of people in the small meeting rooms, in comparison to the base scenario (Fig. 9[c]). Finally, in the third and fourth interventions (MI3, MI4), meeting duration is decreased from 60 min to 30, and 45 min, respectively. In these two interventions, other meeting parameters (meeting room size and the number of participants) are similar to the base scenario. As illustrated in Fig. 9(d), the CIR of the meeting rooms is slightly reduced in MI3, as compared to the base scenario. Additionally, reducing the meeting duration to 30 min (i.e., MI4) lowers the CIR further, as shown in Fig. 9(d). The average daily infection rate for the four interventions is calculated through 100 simulations and presented in Fig. 10.

Simulation results reveal that MI4 has the lowest infection rate among the four meeting interventions, although the impact of all four interventions is very slight (9.8% for MI4). Regarding MI1, Considering that conference rooms already exist in the original office layout (i.e., base scenario), this intervention is rated as a *low*-cost intervention. However, since implementing MI2, MI3, and MI4 requires changes to the employees' behavior, these interventions are rated as *medium*-cost interventions. Furthermore, according to the t-test results, the impact of all meeting interventions on the average infection rate is statistically significant except for MI3 (Table 4).

5.4. Workspace allocation and working shifts

Previous research confirms that COVID-19 transmission significantly increases as the population density in indoor environments increases. Hence, we expect to reduce the average infection rate and CIR by increasing the workspace allocation (i.e., reducing the population density) in this case study. This hypothesis is tested by (1) reducing

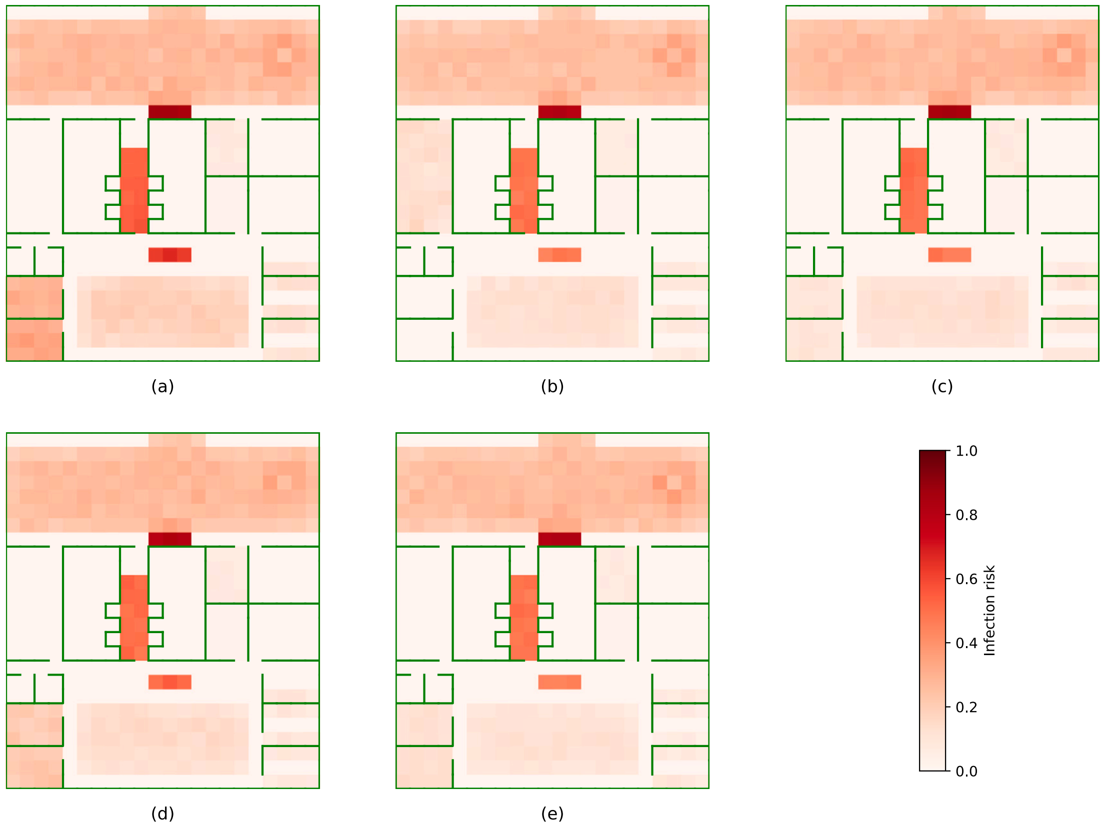

Fig. 9. The impact of meeting interventions on the CIR for (a) Base, (b) MI1, (c) MI2, (d) MI3, (e) MI4.

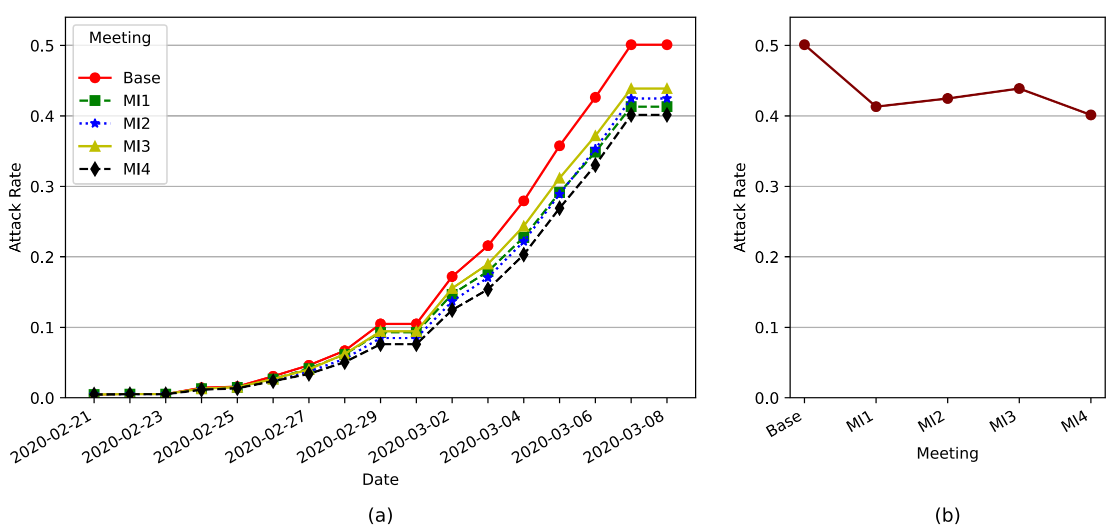

Fig. 10. The impact of meeting interventions on the average daily infection rate.

Table 4
Summary of simulation results for meeting interventions.

Scenario	Room size (m^2)	Meeting size (people)	Duration (min)	Avg. CIR	Avg. infection rate	t-value	Statistical significance
Base	27	16	60	0.112	50.1%	0.000	
MI1	36	16	60	0.092	41.3%	−2.248	Yes
MI2	27	8	60	0.093	42.5%	−1.995	Yes
MI3	27	16	45	0.099	43.9%	−1.565	No
MI4	27	16	30	0.091	40.1%	−2.668	Yes

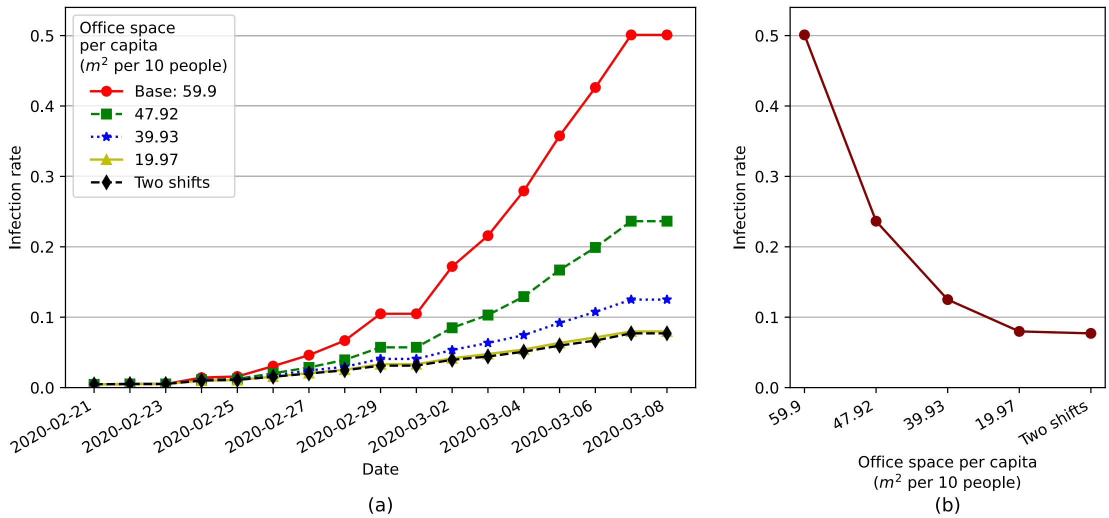

Fig. 11. The effectiveness of increasing the working shifts and increasing the total office space per capita (reducing the population density) on average infection rate.

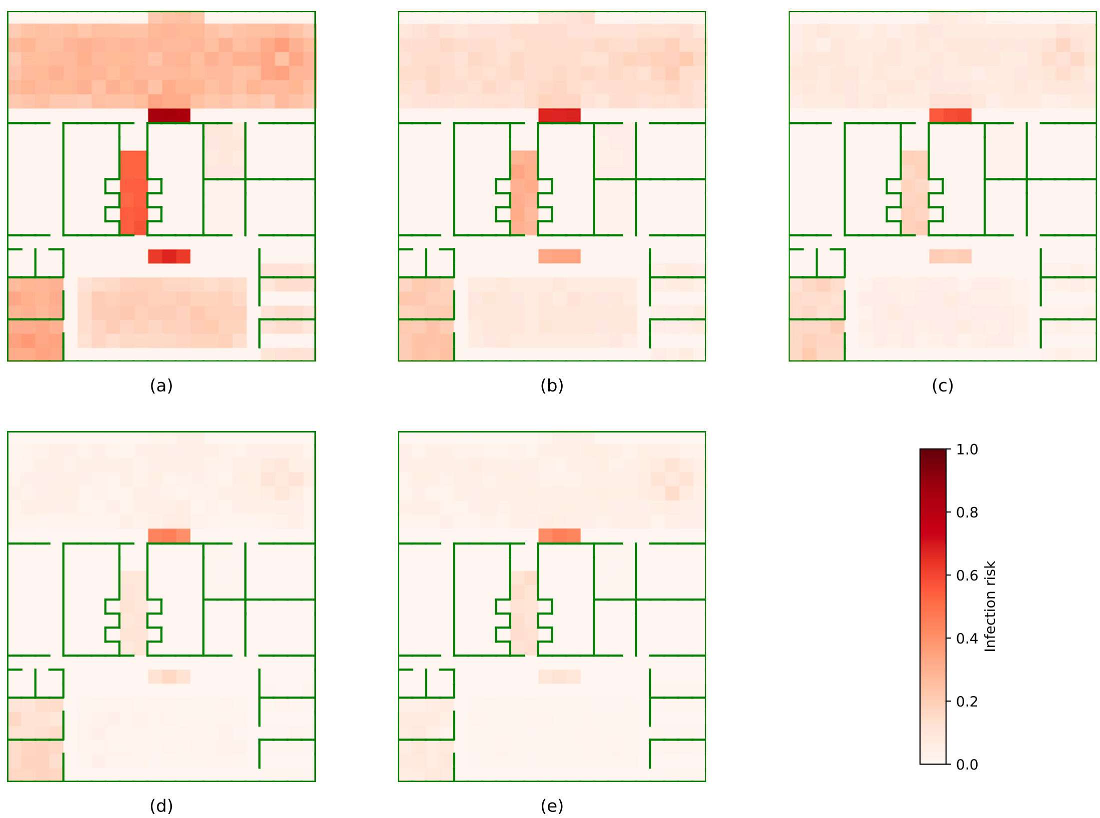

Fig. 12. The impact of workspace allocation on the CIR for (a) Base: 59.9, (b) 47.9, (c) 39.9, (d) 19.9 (m^2 per 10 people), and (e) two work shifts.

the number of employees and (2) changing the work schedule of the call center into two working shifts.

First, the number of employees is reduced to 80%, 67%, and 50% of the base scenario; hence, the average workspace allocation is increased from 59 (m^2 per 10 people) in the base scenario to 77, 91, and 161 (m^2 per 10 people), respectively. Second, two shifts are introduced, each running for 7 h, where each shift runs with half of the employees. The simulation results for the average infection rate are presented in Fig. 11. Also, Fig. 12 shows the impact of these two interventions on reducing the CIR in the case study.

The simulation results confirm that increasing the workspace allocation (i.e., decreasing the population density) significantly reduces the average infection rate, as compared to the base scenario. Furthermore, adding one shift to the work schedule resembles doubling the workspace allocation. Additionally, the t-test results presented in (Table 5) confirm the statistical significance of these interventions' impact on the average infection rate.

Despite the significant impact of these interventions, increasing the workspace allocation and adding one work shift requires significant changes in the spatial structure of the office (i.e., increasing the size) or the work behavior of the employees. Hence, this intervention is rated as a *high*-cost intervention and will be suggested only if implementing *low*- and *medium*-cost interventions are insufficient for improving occupational safety in the office space.

Table 5
Summary of simulation results for changing the workspace allocation and work schedule.

Office space (m^2 per 10 people)	Number of employees	Number of shifts	Avg. CIR	Avg. infection rate	t-value	Statistical significance
59.90	216	1	0.112	50.1%	0.000	
47.92	173	1	0.056	23.6%	−7.540	Yes
39.93	144	1	0.032	12.5%	−11.983	Yes
19.97	108	1	0.021	8.0%	−14.102	Yes
19.97	216	2	0.019	7.7%	−14.040	Yes

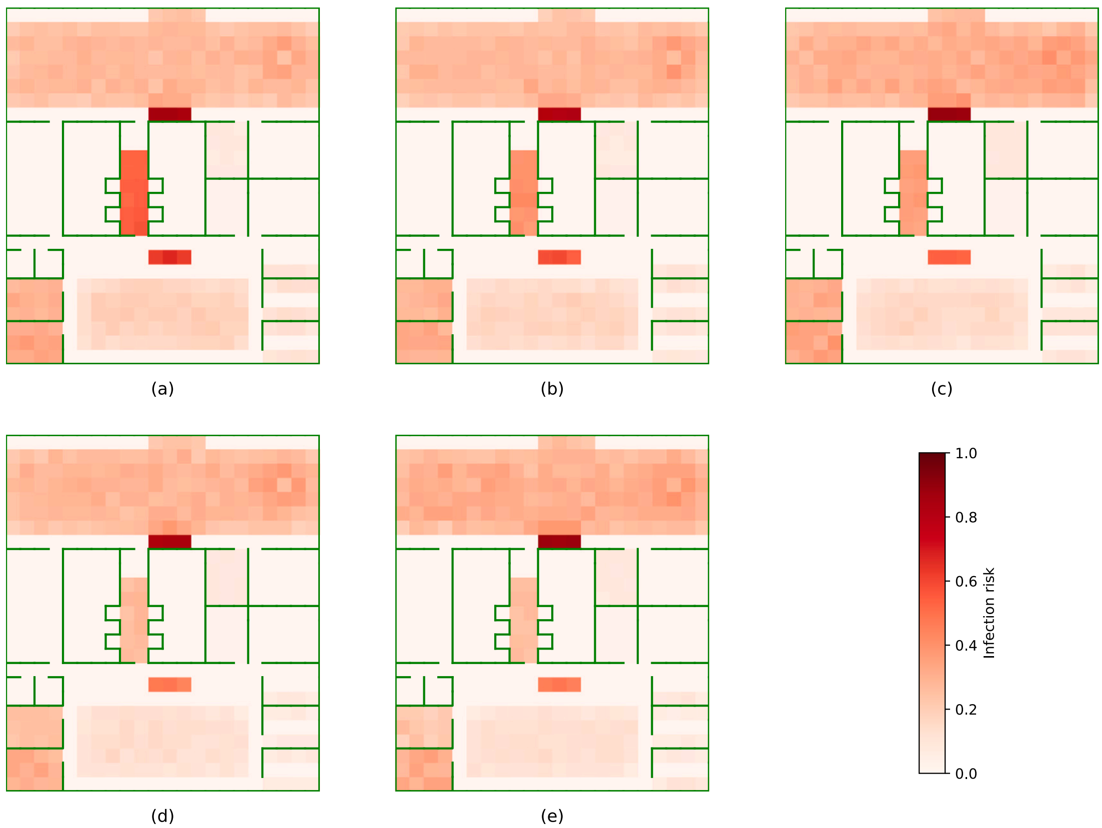

Fig. 13. The impact of permissible time window allocation on CIR for (a) Base (0 min), (b) 30, (c) 60, (d) 120, and (e) 180.

5.5. Allocating permissible time window to start working

The simulation results in the base scenario (Fig. 2[b]) confirm that the elevators' hall is a high-risk zone in the office layout. To address this issue, the population density in the elevators' hall is reduced by allocating a 30 permissible time window to start the workday and gradually increasing it to 60, 120, and 180 min. By implementing this intervention, we are allowing (not mandating) the employees to start their work anytime during the allocated time window and leave the office after completing their 7 h of daily work. For example, for a 30 min permissible time window, the employees are allowed to start working anytime from 9:30 AM to 10:00 AM. In all scenarios, employees arrive at the office within 15 min, before starting their workday; and leave the office within 15 min, after finishing their workday.

Allocating a permissible time window and prolonging it reduce the population density in the elevators' hall since not all employees start and finish their work day simultaneously. Hence, this intervention is supposed to reduce the CIR in the elevators' hall. The simulation results presented in Fig. 13 confirm this hypothesis since the CIR gradually decreases as the permissible time window prolongs.

The average infection rate is predicted for all four scenarios of allocating a permissible time window, and results indicate that allocating a permissible time window of 120 (min) results in the lowest average infection rate (see Fig. 14). However, this intervention, in all four scenarios, has a very slight impact on the average infection rate, and the t-test results – presented in Table 6 – show that this impact is not statistically significant.

Table 6
Summary of simulation results for time-window interventions.

Arrival time window (min)	Avg. CIR	Avg. infection rate	t-value	Stat. significance
Base	0.112	50.1%	0.000	
30	0.105	46.2%	−0.964	No
60	0.111	50.0%	−0.039	No
120	0.099	44.1%	−1.538	No
180	0.103	46.9%	−0.830	No

Additionally, allocating a permissible time window requires some adjustments to the work behavior of the employees; hence, it is rated as a *medium*-cost intervention, and its cost increases as the time window prolongs. Considering its *medium* implementation cost and (statistically) non-significant impact on the average infection rate, this intervention is not used for improving occupational safety in office spaces.

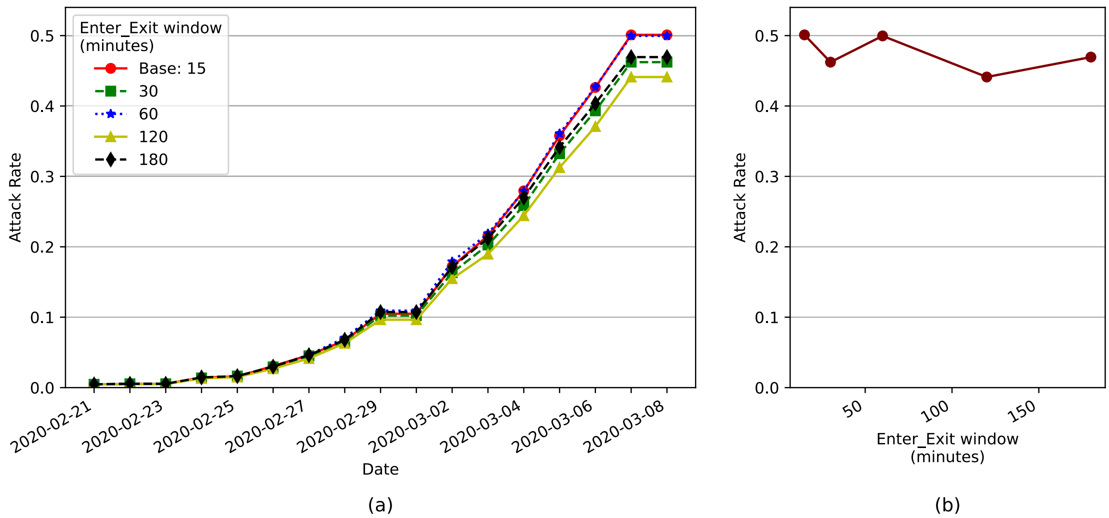

Fig. 14. The effectiveness of increasing the arrival and leaving time window.

6. Improving occupation safety in office spaces

In this section, the most effective non-restrictive interventions introduced and analyzed in Section 5 are implemented to improve occupational safety in the case study. In this process, all interventions rated as *low*- or *medium*-cost are sequentially applied – each sequence is called an evolution – to the case study. The interventions are selected based on their impact zone to avoid redundancy (i.e., not implementing two interventions that target the same high-risk zone), and applied in three evolutions:

- Evolution 1: Increasing the decompression area allocation to 2.60 m^2 per 10 people (see Section 5.2).
- Evolution 2: Changing the workspace setting from open to the clustered workspace with the average cluster size of $ACS = 6.6$ people (see Section 5.1).
- Evolution 3: Decreasing meetings' duration to 30 min (see Section 5.3).

For these three evolutions, the average daily infection rate and the mapping of CIRs over the office layout are presented in Figs. 15 and 16, respectively. In Fig. 15, the gradual decrease of infection rates by adding one intervention at a time confirms the effectiveness of each and every evolution. Additionally, Fig. 16 shows how combining interventions with different impact zones can reduce the CIRs in the entire office layout.

To further investigate the combined effect of these interventions, the statistical significance of each evolution's alleviating impact is tested by t-test. To this end, the average infection rate in each evolution (i) is compared to the previous evolution ($i-1$), to determine whether each evolution is significantly effective or not. Accordingly, the t-test results presented in Table 7 compare the average infection rate of Evolution 1 to the base scenario, Evolution 2 to Evolution 1, and Evolution 3 to Evolution 2. The results confirm that the impacts of all three evolutions are statistically significant in improving occupational safety in office spaces.

Finally, we compare the collective impact of these three interventions (i.e., Evolution 3) to the *high*-cost intervention of adding working shifts and the face mask and vaccination mandates. These two globally accepted interventions, face mask, and vaccination mandates are restrictive; hence, they faced public resistance in different countries (Dror et al., 2020; Kearney et al., 2022; Martin & Vanderslott, 2022). Accordingly, this comparison shows whether our proposed non-restrictive interventions can replace these restrictive ones in the future. The daily infection rate of COVID-19 in these four scenarios (i.e., Evolution 3, adding working shift, face mask mandate, vaccination mandate) is simulated by CoDiSS over 100 simulation runs and the results are presented in Fig. 17.

Table 7
Summary of simulation results for combining different interventions.

Intervention	Avg. CIR	Avg. infection rate	t-value	Statistical significance
Base	0.112	50.1%	0.000	
Evolution 1	0.066	23.3%	−7.550	Yes
Evolution 2	0.033	11.8%	−4.706	Yes
Evolution 3	0.023	7.5%	−2.865	Yes

To accurately simulate the impact of these two interventions, the rate of public compliance with the mandates (in the United Kingdom) and their effectiveness of each are extracted from the literature. An extensive interview survey in Ireland Kearney et al. (2022) with 11,171 participants reveals that 67.3% of the respondents used face masks in shops and supermarkets, and only 17.8% consistently used face masks at work. Additionally, the effectiveness of surgical masks, the most common type used during the COVID-19 pandemic, is [42 – 88%] (Sankhyan et al., 2021). According to the Office for National Statistics (Office of National Statistics, 2023), 70.2% of eligible British citizens are fully vaccinated against COVID-19, and the aggregated effectiveness of vaccines provided to the public is [50−60%] in preventing severe cases of COVID-19 (Agency, 2023). Furthermore, CoDiSS accounts for the decrease in the viral load of the disease in vaccinated vs. non-vaccinated individuals, where the viral load of COVID-19 decreases by 4.8 folds in vaccinated individuals (Puhach et al., 2022).

According to the simulation results, the combined impact of three non-restrictive interventions in Evolution 3 is higher than the effectiveness of using face masks in the office, while the former requires no compliance from the employees and does not alter their work behavior. Additionally, Evolution 3 can improve occupational safety to the same extent as adding one working shift to the case study, though with significantly lower implementation costs. Adding one working shift requires significant changes to the working behavior of employees and can significantly increase the operational costs and energy consumption of the office. However, the three non-restrictive interventions combined (i.e., Evolution 3) can be implemented in similar offices with some simple changes to the layout and slight behavioral changes (i.e., meetings).

The vaccination mandate has a lower infection rate than Evolution 3, which is due to the immunity produced by the vaccine and the lower viral load of COVID-19 in vaccinated individuals. However, vaccination

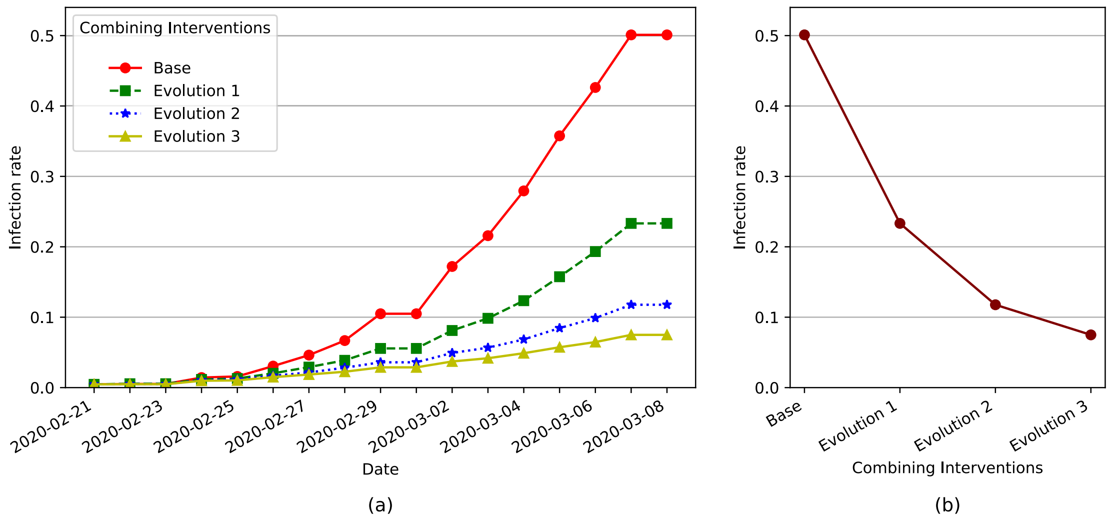

Fig. 15. Gradual improvement of the infection rate by combining interventions.

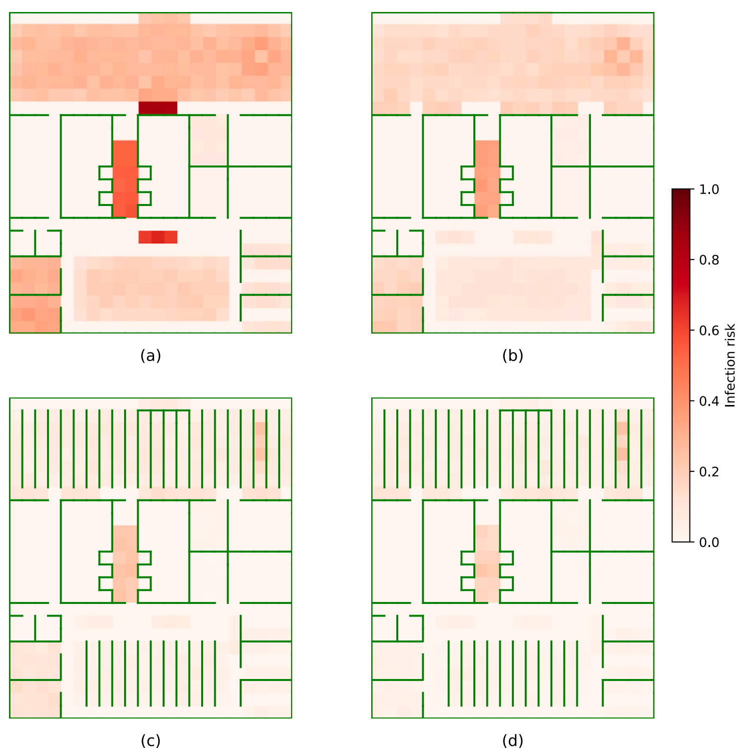

Fig. 16. Gradual improvement of CIR in the office layout by combining interventions (a) Base, (b) Evolution 1, (c) Evolution 2, and (d) Evolution 3.

is a pharmaceutical intervention with high implementation costs on the macro (i.e., research and development) and micro (i.e., people compliance) scales. Additionally, the immunity that COVID-19 vaccines develop in susceptible individuals diminishes over time if booster doses are not received; hence, these simulation results are only valid until the compliance rate and effectiveness of the vaccines are within the given range in Fig. 4. Considerably, the compliance rate used in this paper corresponds to the vaccination program administered in the United Kingdom, which is a pioneer in COVID-19 vaccine development and has one of the highest rates of vaccination (Pettersson, Manley, Hernandez, McPhillips, & Arias, 2023). Furthermore, developing vaccines for new variants of the disease is time and cost-consuming; thus, vaccination alone cannot guarantee occupational safety in the post-pandemic era. Accordingly, our proposed strategy for improving occupational safety (i.e., Evolution 3) is still a viable option despite its lower effectiveness than vaccination. Given its low implementation costs, our proposed strategy can also be applied in combination with vaccination to control the spread of COVID-19 when new variants of the disease emerge.

7. Conclusions and future works

The COVID-19 pandemic has raised concerns regarding the resilience of businesses against the spread of infectious diseases. Several existing interventions for COVID-19 (e.g., face masks, vaccination, social distancing) are associated with high socio-economic costs; hence, for healthy recovery of the economy, non-restrictive interventions are needed to improve occupational safety in office spaces by limiting the spread of COVID-19. This study addressed this need by suggesting, evaluating, and combining several non-restrictive interventions to limit the spread of COVID-19 in office spaces. The effectiveness of these

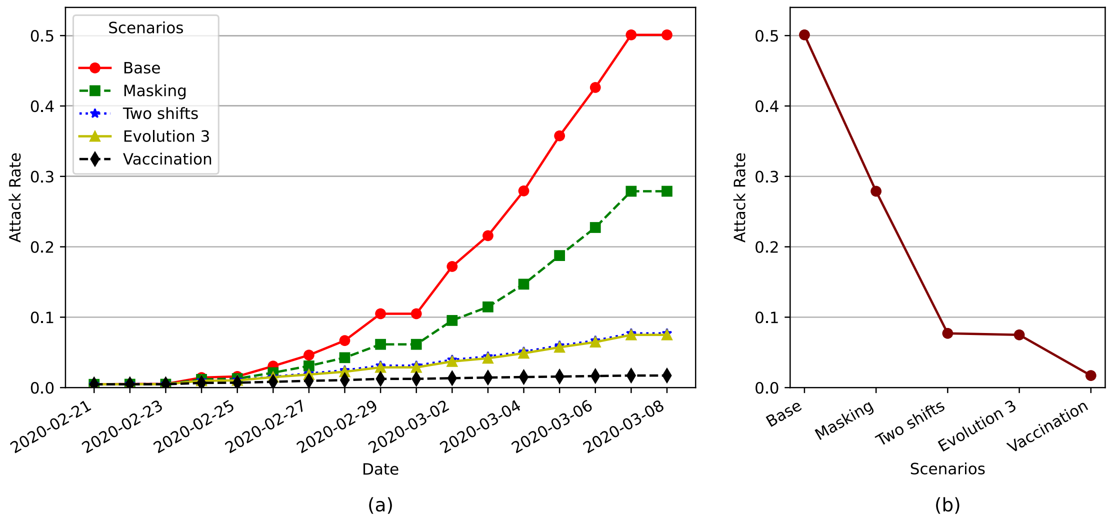

Fig. 17. Comparing the collective impact of interventions in Evolution 3 with two shift work schedules, masking, and vaccination.

interventions is tested by CoDiSS, an agent-based modeling framework developed by the authors for simulating the spread of contagious diseases in buildings.

In order to validate the effectiveness of CoDiSS, we have successfully conducted two approaches. Firstly, a case study was carried out to assess the model's ability to generate results that closely align with actual data. The results obtained from this study demonstrated a high degree of similarity between the model's outputs and the real-world data, indicating the accuracy of CoDiSS. Furthermore, the results obtained from different interventions applied to the framework in Section 5 confirmed that CoDiSS delivers reliable and consistent outcomes across a range of interventions, further highlighting its effectiveness.

The study introduces eight non-restrictive interventions. The results of our analysis show that decompression areas, open workspaces, the elevators hall, and meeting rooms are the hotspots of COVID-19 transmission (i.e., areas with the highest cell infection risk [CIR]). Additionally, our analysis shows that the top three non-restrictive interventions for limiting the spread of COVID-19 are: (I) increasing the number of working shifts; (II) increasing decompression space allocation; and (III) changing the workspace settings from open to a clustered workspace with an average cluster size (ACS) of ≤6.60 people.

Next, we utilized our evaluation results and combined several interventions with low or $medium$ implementation costs to improve occupational safety in office spaces. This is achieved by selecting interventions one at a time based on three criteria (I) the statistical significance of its impact on limiting COVID-19 spread, (II) its implementation cost, and (III) the exclusiveness of its impact zone in the office layout. Hence, the following interventions are selected and sequentially applied to the case study: (I) increasing decompression space allocation, (II) changing workspace settings from an open workspace to a clustered workspace with $ACS = 6.60$; and (III) decreasing meetings duration to 30 min. The simulation results reveal that these interventions, combined, can reduce the infection rate of COVID-19 in the call center (case study) from 50% to 7.5%. The simulation results also indicate that the collective impact of these interventions is higher than using face masks and is equally effective as adding one working shift. Additionally, given their low and $mdium$ implementation costs, these interventions can be easily applied to different office spaces to improve occupational safety in work environments.

The simulation results demonstrate that safe and effective vaccines are more efficient than the non-restrictive interventions introduced. However, it is important to consider that the development, distribution, and administering of vaccine programs are associated with high social and economic costs, and developing new vaccines can be time-consuming, particularly in the case of emerging variants. The vaccination mandate may face resistance from some segments of the population, and, as a consequence, a low compliance rate can limit the effectiveness of vaccines. Additionally, the immunity provided by COVID-19 vaccines diminishes over time, and some individuals may delay receiving their subsequent doses (boosters); consequently, lowered immunity rate may reduce the effectiveness of vaccine intervention. Therefore, a multi-pronged approach that includes a combination of effective interventions, as proposed in this paper, along with vaccines, can be the most viable strategy for improving occupational safety in the post-pandemic era.

The contributions of this paper are threefold. First, a highly granular micro-level framework – CoDiSS – is used for the prognostic analysis of COVID-19 spread in office spaces. This framework addresses several parameters that affect the spread of COVID-19, including virus quanta and its impact on infection probabilities, as well as the changes in the viral load over the entire infection period. Second, through diagnostic analysis, this paper identifies the high-risk zones of COVID-19 transmission in office spaces by mapping the risk of infection on the entire layout of the case study. Third, several non-restrictive interventions are introduced to address COVID-19 transmission in the identified high-risk zones, and the effectiveness of each intervention is tested through simulation. Consequently, the most effective non-restrictive interventions for limiting the spread of COVID-19 are combined, and a strategy is suggested to enhance occupational safety in office spaces in the post-pandemic era. In the presented case study, our suggested strategy reduces the infection rate of COVID-19 from 50.1% to 7.5%.

Although this paper provides a methodological contribution to modeling the spread of COVID-19 and promising results in limiting its spread in office spaces, it has some theoretical and applied limitations. The theoretical limitation of this research relates to CoDiSS (i.e., the ABM framework) since it only addresses the aerosol transmission of contagious diseases and ignores all other transmission routes. Expanding the scope of CoDiSS to encompass the transmission of infectious diseases through droplets and fomite can augment its utility for managing a broad range of infectious diseases. Although in the case of COVID-19, the impact of such improvements will be minor since aerosol is the dominant transmission route of COVID-19.

Additionally, while the results of the study provide valuable insights into potential strategies for improving occupational safety, it is important to note that the interventions described in this paper were tested in a single but typical office space. Therefore, their generalizability to other settings may be limited. Further research is necessary to determine how these interventions can be adapted and modified to suit the unique characteristics of different workplaces, such as modeling the infection spread across multiple floors or inside the co-work and hot-desk workspaces, where individuals are not assigned to a permanent location. Additionally, the impact of several random variables on the spread of COVID-19 may be tested in future research, including the location of the initially infected individual and the occupants' tasks schedule. Implementing the proposed methodology in individual buildings is recommended to identify the most effective interventions for a specific workplace and its unique building layout. This approach enables a more tailored strategy to improve occupational safety that considers the unique spatial and temporal characteristics of each workplace. Future studies could also explore the cost of different interventions in greater detail. By considering both the financial cost and feasibility of adherence, researchers can provide a more comprehensive understanding of implementing the suggested interventions. By taking this approach, interventions can be targeted and optimized to provide the greatest impact, ultimately reducing the spread of infections and improving the overall safety of each workplace.

Declaration of competing interest

The authors declare that they have no known competing financial interests or personal relationships that could have appeared to influence the work reported in this paper.

Data availability

The program code generated for this article, the data used, and all the results are available on the open-access CoDiSS library, the GitHub project cited in the article.

References

Afacan, Y., & Gurel, M. O. (2015). Public toilets: an exploratory study on the demands, needs, and expectations in Turkey. *Environment and Planning B: Planning and Design*, *42*(2), 242–262. http://dx.doi.org/10.1068/b130020p.

Afshar-Nadjafi, B., & Niaki, S. T. A. (2021). Seesaw scenarios of lockdown for COVID-19 pandemic: Simulation and failure analysis. *Sustainable Cities and Society*, *73*, Article 103108. http://dx.doi.org/10.1016/j.scs.2021.103108.

Agency, U. H. S. (2023). Monitoring reports of the effectiveness of COVID-19 vaccination. Last accessed December 2022.

Allen, D. W. (2022). COVID-19 lockdown cost/benefits: A critical assessment of the literature. *International Journal of the Economics of Business*, *29*(1), 1–32. http://dx.doi.org/10.1080/13571516.2021.1976051.

Araya, F. (2021a). Modeling the spread of COVID-19 on construction workers: An agent-based approach. *Safety Science*, *133*, Article 105022. http://dx.doi.org/10.1016/j.ssci.2020.105022.

Araya, F. (2021b). Modeling working shifts in construction projects using an agent-based approach to minimize the spread of COVID-19. *Journal of Building Engineering*, *41*, Article 102413. http://dx.doi.org/10.1016/j.jobe.2021.102413.

Arena, A., Altieri, M., Filipponi, F., Degli Esposti, E., Franceschini, C., Virgilio, A., et al. (2022). When two coincidences are a clue: A retrospective cohort study regarding the incidence of ruptured tubal pregnancies in a northern Italy hospital during the COVID-19-19 pandemic. *Clinical and Experimental Obstetrics & Gynecology*, *49*(11), 251. http://dx.doi.org/10.31083/j.ceog4911251.

Aylett-Bullock, J., Cuesta-Lazaro, C., Quera-Bofarull, A., Katta, A., Hoffmann Pham, K., Hoover, B., et al. (2021). Operational response simulation tool for epidemics within refugee and IDP settlements: A scenario-based case study of the cox's bazar settlement. *PLoS Computational Biology*, *17*(10), Article e1009360. http://dx.doi.org/10.1371/journal.pcbi.1009360.

Bandyopadhyay, S., & Bhattacharya, R. (2014). *Discrete and continuous simulation: theory and practice*. CRC Press.

Bazzoli, A., & Probst, T. M. (2022). COVID-19 moral disengagement and prevention behaviors: The impact of perceived workplace COVID-19 safety climate and employee job insecurity. *Safety Science*, *150*, Article 105703. http://dx.doi.org/10.1016/j.ssci.2022.105703.

Berry, G., Parsons, A., Morgan, M., Rickert, J., & Cho, H. (2022). A review of methods to reduce the probability of the airborne spread of COVID-19 in ventilation systems and enclosed spaces. *Environmental Research*, *203*, Article 111765. http://dx.doi.org/10.1016/j.envres.2021.111765.

Bhagat, R. K., Wykes, M. D., Dalziel, S. B., & Linden, P. (2020). Effects of ventilation on the indoor spread of COVID-19. *Journal of Fluid Mechanics*, *903*, F1. http://dx.doi.org/10.1017/jfm.2020.720.

Blasche, G., Pasalic, S., Bauböck, V.-M., Haluza, D., & Schoberberger, R. (2017). Effects of rest-break intention on rest-break frequency and work-related fatigue. *Human Factors*, *59*(2), 289–298. http://dx.doi.org/10.1177/0018720816671605.

Bo, Y., Guo, C., Lin, C., Zeng, Y., Li, H. B., Zhang, Y., et al. (2021). Effectiveness of non-pharmaceutical interventions on COVID-19 transmission in 190 countries from 23 january to 13 april 2020. *International Journal of Infectious Diseases*, *102*, 247–253. http://dx.doi.org/10.1016/j.ijid.2020.10.066.

Borshchev, A. (2013). *The big book of simulation modeling: multimethod modeling with anylogic 6*. AnyLogic North America.

Buonanno, G., Stabile, L., & Morawska, L. (2020). Estimation of airborne viral emission: Quanta emission rate of SARS-CoV-2 for infection risk assessment. *Environment International*, *141*, Article 105794. http://dx.doi.org/10.1016/j.envint.2020.105794.

Che, W., Ding, J., & Li, L. (2022). Airflow deflectors of external windows to induce ventilation: Towards COVID-19 prevention and control. *Sustainable Cities and Society*, *77*, Article 103548. http://dx.doi.org/10.1016/j.scs.2021.103548.

Choi, S., & Yoon, S. (2023). Energy signature-based clustering using open data for urban building energy analysis toward carbon neutrality: A case study on electricity change under COVID-19. *Sustainable Cities and Society*, Article 104471. http://dx.doi.org/10.1016/j.scs.2023.104471.

Chu, J. (2021). A statistical analysis of the novel coronavirus (COVID-19) in Italy and Spain. *PLoS One*, *16*(3), Article e0249037. http://dx.doi.org/10.1371/journal.pone.0249037.

Corbaz-Kurth, S., Juvet, T. M., Benzakour, L., Cereghetti, S., Fournier, C.-A., Moullec, G., et al. (2022). How things changed during the COVID-19 pandemic's first year: A longitudinal, mixed-methods study of organisational resilience processes among healthcare workers. *Safety Science*, *155*, Article 105879. http://dx.doi.org/10.1016/j.ssci.2022.105879.

de Oliveira, P. M., Mesquita, L. C., Gkantonas, S., Giusti, A., & Mastorakos, E. (2021). Evolution of spray and aerosol from respiratory releases: theoretical estimates for insight on viral transmission. *Proceedings of the Royal Society of London, Series A (Mathematical and Physical Sciences)*, *477*(2245), Article 20200584. http://dx.doi.org/10.1098/rspa.2020.0584.

Dempsey, P. C., Musicha, C., Rowlands, A. V., Davies, M., Khunti, K., Razieh, C., et al. (2022). Investigation of a UK biobank cohort reveals causal associations of self-reported walking pace with telomere length. *Communications Biology*, *5*(1), 381. http://dx.doi.org/10.1038/s42003-022-03323-x.

Dicker, R. C., Coronado, F., Koo, D., & Parrish, R. G. (2012). *Principles of epidemiology in public health practice; an introduction to applied epidemiology and biostatistics*. Atlanta, GA: U.S. Department of Health and Human Services.

Dror, A. A., Eisenbach, N., Taiber, S., Morozov, N. G., Mizrachi, M., Zigron, A., et al. (2020). Vaccine hesitancy: the next challenge in the fight against COVID-19. *European Journal of Epidemiology*, *35*, 775–779. http://dx.doi.org/10.1007/s10654-020-00671-y.

Fang, L., Karakiulakis, G., & Roth, M. (2020). Are patients with hypertension and diabetes mellitus at increased risk for COVID-19 infection? *The Lancet Respiratory Medicine*, *8*(4), Article e21. http://dx.doi.org/10.1016/S2213-2600(20)30116-8.

Flaxman, S., Mishra, S., Gandy, A., Unwin, H. J. T., Mellan, T. A., Coupland, H., et al. (2020). Estimating the effects of non-pharmaceutical interventions on COVID-19 in europe. *Nature*, *584*(7820), 257–261. http://dx.doi.org/10.1038/s41586-020-2405-7.

Gerami-Seresht, N., & Sadeghi, N. (2023). Contagious disease spread simulator. https://github.com/Project-CoDiSS.

González-Torres, M., Pérez-Lombard, L., Coronel, J. F., Maestre, I. R., & Yan, D. (2022). A review on buildings energy information: Trends, end-uses, fuels and drivers. *Energy Reports*, *8*, 626–637. http://dx.doi.org/10.1016/j.egyr.2021.11.280.

Goyal, A., Reeves, D. B., Cardozo-Ojeda, E. F., Schiffer, J. T., & Mayer, B. T. (2021). Viral load and contact heterogeneity predict SARS-CoV-2 transmission and super-spreading events. *Elife*, *10*, Article e63537. http://dx.doi.org/10.7554/eLife.63537.

Guessoum, S. B., Lachal, J., Radjack, R., Carretier, E., Minassian, S., Benoit, L., et al. (2020). Adolescent psychiatric disorders during the COVID-19 pandemic and lockdown. *Psychiatry Research*, *291*, Article 113264. http://dx.doi.org/10.1016/j.psychres.2020.113264.

IEA (2022). Buildings. Last accessed December 2022.

Jadidi, M., Jamshidiha, S., Masroori, I., Moslemi, P., Mohammadi, A., & Pourahmadi, V. (2021). A two-step vaccination technique to limit COVID-19 spread using mobile data. *Sustainable Cities and Society*, *70*, Article 102886. http://dx.doi.org/10.1016/j.scs.2021.102886.

Jiang, G., Wang, C., Song, L., Wang, X., Zhou, Y., Fei, C., et al. (2021). Aerosol transmission, an indispensable route of COVID-19 spread: case study of a department-store cluster. *Frontiers of Environmental Science & Engineering*, *15*, 1–12. http://dx.doi.org/10.1007/s11783-021-1386-6.

Jimenez, J. L., Marr, L. C., Randall, K., Ewing, E. T., Tufekci, Z., Greenhalgh, T., et al. (2022). What were the historical reasons for the resistance to recognizing airborne transmission during the COVID-19 pandemic? *Indoor Air*, *32*(8), Article e13070. http://dx.doi.org/10.1111/ina.13070.

Katal, A., Wang, L. L., & Albettar, M. (2022). A real-time web tool for monitoring and mitigating indoor airborne COVID-19 transmission risks at city scale. *Sustainable Cities and Society*, *80*, Article 103810. http://dx.doi.org/10.1016/j.scs.2022.103810.

Kearney, P. M., Spillane, M., Humphries, R., Gannon, A., Stamenic, D., Bhuachalla, C. N., et al. (2022). Compliance with local travel restrictions and face masks during first phase of COVID-19 pandemic in Ireland: a national survey. *Journal of Public Health (Oxford, England)*, http://dx.doi.org/10.1093/pubmed/fdac017.

Kerr, C. C., Stuart, R. M., Mistry, D., Abeysuriya, R. G., Rosenfeld, K., Hart, G. R., et al. (2021). Covasim: an agent-based model of COVID-19 dynamics and interventions. *PLoS Computational Biology*, *17*(7), Article e1009149. http://dx.doi.org/10.1371/journal.pcbi.1009149.

Khan, A. H., Tirth, V., Fawzy, M., Mahmoud, A. E. D., Khan, N. A., Ahmed, S., et al. (2021). COVID-19 transmission, vulnerability, persistence and nanotherapy: a review. *Environmental Chemistry Letters*, *19*(4), 2773–2787. http://dx.doi.org/10.1007/s10311-021-01229-4.

Krebs, T., von Jouanne-Diedrich, H., & Moeckel, M. J. (2021). COVID-19 scenarios for comparing the effectiveness of age-specific vaccination regimes, exemplified for the city of aschaffenburg (Germany). http://dx.doi.org/10.1101/2021.08.31.21262915, medRxiv. 2021-2008.

Krivorotko, O., Sosnovskaia, M., Vashchenko, I., Kerr, C., & Lesnic, D. (2022). Agent-based modeling of COVID-19 outbreaks for new york state and UK: Parameter identification algorithm. *Infectious Disease Modelling*, *7*(1), 30–44. http://dx.doi.org/10.1016/j.idm.2021.11.004.

Lancet, T. (2020). COVID-19: protecting health-care workers. *Lancet (London, England)*, *395*(10228), 922. http://dx.doi.org/10.1016/S0140-6736(20)30644-9.

Latkowski, R., & Dunin-Keplicz, B. (2021). An agent-based COVID-19 simulator: extending covasim to the polish context. *Procedia Computer Science*, *192*, 3607–3616. http://dx.doi.org/10.1016/j.procs.2021.09.134.

Lewis, D., et al. (2022). Why the WHO took two years to say COVID is airborne. *Nature*, *604*(7904), 26–31. http://dx.doi.org/10.1038/d41586-022-00925-7.

Li, J., & Giabbanelli, P. (2021). Returning to a normal life via COVID-19 vaccines in the United States: a large-scale agent-based simulation study. *JMIR Medical Informatics*, *9*(4), Article e27419. http://dx.doi.org/10.2196/27419.

Liao, C., Chen, X., Zhuo, L., Liu, Y., Tao, H., & Burton, C. G. (2022). Reopen schools safely: simulating COVID-19 transmission on campus with a contact network agent-based model. *International Journal of Digital Earth*, *15*(1), 381–396. http://dx.doi.org/10.1080/17538947.2022.2032419.

Liu, Y., Yan, L.-M., Wan, L., Xiang, T.-X., Le, A., Liu, J.-M., et al. (2020). Viral dynamics in mild and severe cases of COVID-19. *The Lancet Infectious Diseases*, *20*(6), 656–657. http://dx.doi.org/10.1016/S1473-3099(20)30232-2.

Martin, S., & Vanderslott, S. (2022). "Any idea how fast 'it's just a mask!'can turn into 'it's just a vaccine!'": From mask mandates to vaccine mandates during the COVID-19 pandemic. *Vaccine*, *40*(51), 7488–7499. http://dx.doi.org/10.1016/j.vaccine.2021.10.031.

Martinez, I., Bruse, J. L., Florez-Tapia, A. M., Viles, E., & Olaizola, I. G. (2022). Arch-abm: An agent-based simulator of human interaction with the built environment. CO2 and viral load analysis for indoor air quality. *Building and Environment*, *207*, Article 108495. http://dx.doi.org/10.1016/j.buildenv.2021.108495.

Mendez-Brito, A., El Bcheraoui, C., & Pozo-Martin, F. (2021). Systematic review of empirical studies comparing the effectiveness of non-pharmaceutical interventions against COVID-19. *Journal of Infection*, *83*(3), 281–293. http://dx.doi.org/10.1016/j.jinf.2021.06.018.

Müller, B., Bohn, F., Dreßler, G., Groeneveld, J., Klassert, C., Martin, R., et al. (2013). Describing human decisions in agent-based models–odd+ d, an extension of the ODD protocol. *Environmental Modelling & Software*, *48*, 37–48. http://dx.doi.org/10.1016/j.envsoft.2013.06.003.

Office of National Statistics (2023). Coronavirus (COVID-19) latest insights: Vaccines. Last accessed December 2022.

Panovska-Griffiths, J., Swallow, B., Hinch, R., Cohen, J., Rosenfeld, K., Stuart, R. M., et al. (2022). Statistical and agent-based modelling of the transmissibility of different SARS-CoV-2 variants in England and impact of different interventions. *Philosophical Transactions of the Royal Society, Series A*, *380*(2233), Article 20210315. http://dx.doi.org/10.1098/rsta.2021.0315.

Park, S. Y., Kim, Y.-M., Yi, S., Lee, S., Na, B.-J., Kim, C. B., et al. (2020). Coronavirus disease outbreak in call center, South Korea. *Emerging Infectious Diseases*, *26*(8), 1666. http://dx.doi.org/10.3201/eid2608.201274.

Park, S.-H., Yook, S.-J., & Koo, H. B. (2022). Natural ventilation and air purification for effective removal of airborne virus in classrooms with heater operation. *Toxics*, *10*(10), 573. http://dx.doi.org/10.3390/toxics10100573.

Pauksztat, B., Andrei, D. M., & Grech, M. R. (2022). Effects of the COVID-19 pandemic on the mental health of seafarers: A comparison using matched samples. *Safety Science*, *146*, Article 105542. http://dx.doi.org/10.1016/j.ssci.2021.105542.

Perra, N. (2021). Non-pharmaceutical interventions during the COVID-19 pandemic: A review. *Physics Reports*, *913*, 1–52. http://dx.doi.org/10.1016/j.physrep.2021.02.001.

Pettersson, H., Manley, B., Hernandez, S., McPhillips, D., & Arias, T. (2023). Tracking COVID-19 vaccination worldwide. Last accessed December 2022.

Puhach, O., Adea, K., Hulo, N., Sattonnet, P., Genecand, C., Iten, A., et al. (2022). Infectious viral load in unvaccinated and vaccinated patients infected with SARS-CoV-2 WT, delta and omicron. http://dx.doi.org/10.1101/2022.01.10.22269010, medRxiv. 2022-2001.

Raoufi, M., & Fayek, A. R. (2021). Identifying actions to control and mitigate the effects of the COVID-19 pandemic on construction organizations: Preliminary findings. *Public Works Management & Policy*, *26*(1), 47–55. http://dx.doi.org/10.1177/1087724X20969164.

Riley, E., Murphy, G., & Riley, R. (1978). Airborne spread of measles in a suburban elementary school. *American Journal of Epidemiology*, *107*(5), 421–432. http://dx.doi.org/10.1093/oxfordjournals.aje.a112560.

Saeedi, S. (2018). Integrating macro and micro scale approaches in the agent-based modeling of residential dynamics. *International Journal of Applied Earth Observation and Geoinformation*, *68*, 214–229. http://dx.doi.org/10.1016/j.jag.2018.02.012.

Sankhyan, S., Heinselman, K. N., Ciesielski, P. N., Barnes, T., Himmel, M. E., Teed, H., et al. (2021). Filtration performance of layering masks and face coverings and the reusability of cotton masks after repeated washing and drying. *Aerosol and Air Quality Research*, *21*(11), Article 210117. http://dx.doi.org/10.4209/aaqr.210117.

Seresht, N. G. (2022). Enhancing resilience in construction against infectious diseases using stochastic multi-agent approach. *Automation in Construction*, *140*, Article 104315. http://dx.doi.org/10.1016/j.autcon.2022.104315.

Shamil, M. S., Farheen, F., Ibtehaz, N., Khan, I. M., & Rahman, M. S. (2021). An agent-based modeling of COVID-19: validation, analysis, and recommendations. *Cognitive Computation*, 1–12. http://dx.doi.org/10.1007/s12559-020-09801-w.

Sheikhnejad, Y., Aghamolaei, R., Fallahpour, M., Motamedi, H., Moshfeghi, M., Mirzaei, P. A., et al. (2022). Airborne and aerosol pathogen transmission modeling of respiratory events in buildings: An overview of computational fluid dynamics. *Sustainable Cities and Society*, Article 103704. http://dx.doi.org/10.1016/j.scs.2022.103704.

Shorfuzzaman, M., Hossain, M. S., & Alhamid, M. F. (2021). Towards the sustainable development of smart cities through mass video surveillance: A response to the COVID-19 pandemic. *Sustainable Cities and Society*, *64*, Article 102582. http://dx.doi.org/10.1016/j.scs.2020.102582.

Silkin, L. (2023). Employment law in the Republic of Korea – an overview. Last accessed December 2022.

van Smeden, M., Reitsma, J. B., Riley, R. D., Collins, G. S., & Moons, K. G. (2021). Clinical prediction models: diagnosis versus prognosis. *Journal of Clinical Epidemiology*, *132*, 142–145. http://dx.doi.org/10.1016/j.jclinepi.2021.01.009.

Tellier, R. (2022). COVID-19: the case for aerosol transmission. *Interface Focus*, *12*(2), Article 20210072. http://dx.doi.org/10.1098/rsfs.2021.0072.

Truszkowska, A., Thakore, M., Zino, L., Butail, S., Caroppo, E., Jiang, Z.-P., et al. (2021). Designing the safe reopening of US towns through high-resolution agent-based modeling. *Advanced Theory and Simulations*, *4*(9), Article 2100157. http://dx.doi.org/10.1002/adts.202100157.

Verizon (2003). A study of trends, costs, and attitudes toward business travel and teleconferencing, and their impact on productivity. Last accessed December 2022.

Vu, T.-V., Vo-Thanh, T., Nguyen, N. P., Van Nguyen, D., & Chi, H. (2022). The COVID-19 pandemic: Workplace safety management practices, job insecurity, and employees' organizational citizenship behavior. *Safety Science*, *145*, Article 105527. http://dx.doi.org/10.1016/j.ssci.2021.105527.

Wali, B. (2023). Interactive impacts of walkability, social vulnerability, & travel behavior on COVID-19 mortality: A hierarchical Bayesian spatial random parameter approach. *Sustainable Cities and Society*, Article 104454.

Watanabe, T., Bartrand, T. A., Weir, M. H., Omura, T., & Haas, C. N. (2010). Development of a dose-response model for SARS coronavirus. *Risk Analysis: An International Journal*, *30*(7), 1129–1138. http://dx.doi.org/10.1111/j.1539-6924.2010.01427.x.

Xie, G. (2020). A novel Monte Carlo simulation procedure for modelling COVID-19 spread over time. *Scientific Reports*, *10*(1), 13120. http://dx.doi.org/10.1038/s41598-020-70091-1.

Zhao, X., Liu, S., Yin, Y., Zhang, T., & Chen, Q. (2022). Airborne transmission of COVID-19 virus in enclosed spaces: An overview of research methods. *Indoor Air*, *32*(6), Article e13056. http://dx.doi.org/10.1111/ina.13056.